bioRxiv preprint doi: https://doi.org/10.1101/002907; this version posted February 21, 2014. The copyright holder for this preprint (which was not certified by peer review) is the author/funder, who has granted bioRxiv a license to display the preprint in perpetuity. It is made available under aCC-BY-NC-ND 4.0 International license.

Population diversification in a yeast metabolic program promotes anticipation of environmental shifts

Ophelia S. Venturelli[1,2,3], Ignacio Zuleta[2,3], Richard M. Murray[1], Hana El-Samad[2,3*]

[1]Division of Biology and Biological Engineering, California Institute of Technology, Pasadena, California, 91125
[2]Department of Biochemistry and Biophysics, University of California San Francisco, San Francisco, California, 94158
[3]The California Institute for Quantitative Biosciences, University of California San Francisco, San Francisco, California, 94158

*To whom correspondence should be addressed: hana.el-samad@ucsf.edu

bioRxiv preprint doi: https://doi.org/10.1101/002907; this version posted February 21, 2014. The copyright holder for this preprint (which was not certified by peer review) is the author/funder, who has granted bioRxiv a license to display the preprint in perpetuity. It is made available under aCC-BY-NC-ND 4.0 International license.

ABSTRACT

Delineating the strategies by which cells contend with combinatorial changing environments is crucial for understanding cellular regulatory organization. When presented with two carbon sources, microorganisms first consume the carbon substrate that supports the highest growth rate (e.g. glucose) and then switch to the secondary carbon source (e.g. galactose), a paradigm known as the Monod model. Sequential sugar utilization has been attributed to transcriptional repression of the secondary metabolic pathway, followed by activation of this pathway upon depletion of the preferred carbon source. In this work, we challenge this notion. Although *Saccharomyces cerevisiae* cells consume glucose before galactose, we demonstrate that the galactose regulatory pathway is activated in a fraction of the cell population hours before glucose is fully consumed. This early activation reduces the time required for the population to transition between the two metabolic programs and provides a fitness advantage that might be crucial in competitive environments. Importantly, these findings define a new paradigm for the response of microbial populations to combinatorial carbon sources.

bioRxiv preprint doi: https://doi.org/10.1101/002907; this version posted February 21, 2014. The copyright holder for this preprint (which was not certified by peer review) is the author/funder, who has granted bioRxiv a license to display the preprint in perpetuity. It is made available under aCC-BY-NC-ND 4.0 International license.

1 **INTRODUCTION**

2 Microbial cells are continuously bombarded by diverse and changing combinatorial
3 environmental stimuli. To survive and reproduce, a cell must accurately detect, assess, and
4 selectively respond to these signals. Specifically, in competitive and unpredictable
5 environments, cells need to constantly integrate information about the nature and
6 quantities of nutritional substrates to scavenge maximum nutritional value[1]. Organisms
7 that can balance the anticipation of future environmental shifts without sacrificing the rate
8 of reproduction by excess metabolic burden exhibit a fitness advantage. However, optimal
9 metabolic strategies for achieving this balance have not been thoroughly explored.

10 Studies of the response of microbial cells to the availability of multiple sugars has a long
11 history, starting with the seminal work of Dienert in yeast[2,3] and Monod in bacteria[4,5].
12 When presented with both glucose and galactose, microbial cells consume these carbon
13 substrates in a sequential manner rather than simultaneously metabolizing both, resulting
14 in two separate growth phases[5]. In the first phase, cells preferentially metabolize the
15 sugar on which they can grow the fastest (glucose in this case). Upon glucose depletion,
16 cells transition to metabolizing the less preferred sugar (galactose). This response,
17 classically known as "catabolite repression", posits that the synthesis of the enzymes
18 needed to metabolize the less preferred sugar is inhibited across the whole population.
19 This inhibition is relieved by depletion of the preferred sugar, which triggers the diauxic
20 shift. Crucially, in this model, the sequential consumption of the two sugars is generally
21 attributed to the sequential expression of the enzymes needed for their metabolism[6].

bioRxiv preprint doi: https://doi.org/10.1101/002907; this version posted February 21, 2014. The copyright holder for this preprint (which was not certified by peer review) is the author/funder, who has granted bioRxiv a license to display the preprint in perpetuity. It is made available under aCC-BY-NC-ND 4.0 International license.

22 In this work, we demonstrate that while *S. cerevisiae* cells indeed undergo sequential sugar
23 consumption in the presence of combinations of glucose and galactose, the synthesis of the
24 enzymes needed for the metabolism of galactose is not necessarily sequential. Specifically,
25 we find that for a large combinatorial space of glucose-galactose inputs, a subpopulation of
26 cells arises where the galactose transcriptional program is induced hours before the
27 depletion of glucose. Intriguingly, these cells have a fully active galactose transcriptional
28 program, yet they do not metabolize this sugar until glucose is exhausted. We demonstrate
29 that this heterogeneous strategy is essential for rapid growth during the metabolic
30 transition from glucose to galactose. These data suggest that the response of
31 microorganisms to combinatorial environments may frequently involve diversification of
32 phenotypes across a population. Furthermore, this strategy integrates direct
33 environmental sensing with an anticipation of future environmental shifts. As such, it
34 constitutes an elaboration on bet-hedging mechanisms that often rely on stochastic
35 fluctuations to produce subpopulations with different phenotypes without a dominant
36 input from the environment[7].

37 **RESULTS**

38 We studied the time-resolved response of a population of yeast cells to combinatorial
39 inputs of glucose and galactose using our automated flow cytometry setup that measures
40 gene expression approximately every 20 min for 14 hours (Fig. 1A)[8]. This technology
41 enabled us to measure the galactose (GAL) pathway activity dynamics in single-cells using
42 the epimerase *GAL10* promoter (pGAL10) driving Venus (YFP) and to dissect the
43 quantitative growth patterns of the microbial culture.

44

bioRxiv preprint doi: https://doi.org/10.1101/002907; this version posted February 21, 2014. The copyright holder for this preprint (which was not certified by peer review) is the author/funder, who has granted bioRxiv a license to display the preprint in perpetuity. It is made available under aCC-BY-NC-ND 4.0 International license.

45 For sufficiently low glucose concentrations, pGAL10 induced as a single monomodal
46 distribution. By contrast, pGAL10 did not activate over the course of the experiment for
47 glucose concentrations significantly higher than those of galactose. These behaviors
48 recapitulate previously observed phenotypes[9,10]. However, for a large spectrum of
49 combinatorial glucose-galactose inputs aggregating around the regime of equal
50 concentration of these two sugars, we observed the emergence of a bimodal gene
51 expression response in which only a fraction of the population induced pGAL10 (Fig. 1A,B).
52 In this regime, bimodality was transient since the cohort of OFF cells uniformly switched
53 ON following a delay. The promoters of the galactokinase *GAL1* (pGAL1), permease
54 transporter *GAL2* (pGAL2) and transferase *GAL7* (pGAL7) exhibited similar gene
55 expression patterns, indicating that this transient bimodality was a general feature of the
56 GAL pathway in response to a mixture of glucose and galactose (Supplementary Fig. 1).
57
58 Stochastic switching between the ON and OFF states in the transient bimodality region
59 would generate a population of cells with intermediate fluorescence levels. This is due to
60 the slow dynamics of protein synthesis and the high stability of fluorescent proteins,
61 resulting in the decay rate of the fluorophore being dominated by dilution after cell division.
62 However, in our data, the ON and OFF subpopulations were clearly separated from each
63 other in the bimodal region and we did not detect cells of intermediate fluorescence values.
64 In addition, for a given dual-sugar input, the fraction of GAL ON cells did not change
65 significantly over time in the bimodality region (highlighted box in Supplementary Fig.
66 2A,B). Taken together with a previous study demonstrating that the GAL system can only
67 exhibit stochastic transitions between states in the absence of the *GAL80* negative feedback

bioRxiv preprint doi: https://doi.org/10.1101/002907; this version posted February 21, 2014. The copyright holder for this preprint (which was not certified by peer review) is the author/funder, who has granted bioRxiv a license to display the preprint in perpetuity. It is made available under aCC-BY-NC-ND 4.0 International license.

68 loop but not in wild type[11], our data indicate that it is unlikely that cells are continuously
69 switching between the ON and OFF states. Therefore, this phenomenon is distinguishable
70 from previously observed stochastic switching between phenotypes[12,13].
71
72 Using a Gaussian mixture model (GMM) to deconvolve the two populations (see Methods),
73 we quantified three measures of the response: the time to early activation for conditions
74 with a detectable early activated population (δ_a), the delay between early and late
75 activation for conditions with transient bimodality (δ_g, highlighted panels), and the fraction
76 of ON cells quantified at the midpoint between the half-max of the early and delayed
77 activation responses ($F_{ON\text{-}mid}$) (Fig. 1B, see Methods). δ_a was modestly increased by glucose
78 and reduced by galactose (Fig. 1C). By contrast, δ_g, showed a substantial linear increase as a
79 function of initial glucose (highlighted panels in Fig. 1A, Fig. 1D). However, δ_g was not
80 significantly modified by the initial galactose concentration (Supplementary Fig. 3A). $F_{ON\text{-}}$
81 $_{mid}$ significantly increased with the initial galactose level and was reduced by the initial
82 glucose concentration for any given concentration of galactose (Fig. 1E). δ_g and $F_{ON\text{-}mid}$ were
83 modified in a set of mutants including regulators of the GAL pathway and glucose
84 repression, suggesting that these phenotypes are modulated by a complex molecular
85 program involving many factors (Supplementary Text, Supplementary Fig. 5A-D).
86
87 The existence of a subpopulation of cells in which the galactose transcriptional pathway
88 was active in the transient bimodality regime suggested that the population might be
89 consuming galactose concurrently with glucose. To test this hypothesis, we measured
90 glucose, galactose and the fraction of ON cells (F_{ON}) as a function of time in response to

bioRxiv preprint doi: https://doi.org/10.1101/002907; this version posted February 21, 2014. The copyright holder for this preprint (which was not certified by peer review) is the author/funder, who has granted bioRxiv a license to display the preprint in perpetuity. It is made available under aCC-BY-NC-ND 4.0 International license.

91 0.1% glucose and 0.1% galactose, a condition in which the population exhibits a bimodal
92 response. While these data recapitulated the known sequential order of sugar utilization,
93 F_{ON} increased immediately following the dual-sugar stimulus and transiently plateaued
94 before the cells consumed the available glucose (highlighted box in Fig. 2A and
95 Supplementary Fig. 2). The initial concentration of glucose determined the duration of this
96 plateau (Supplementary Fig. 2C). F_{ON} underwent a second increase to approximately 100%
97 precisely at the time of total glucose depletion. Therefore, the timing of the delayed
98 activation of the repressed subpopulation, and consequently the magnitude of δ_g, seemed
99 to be determined by the time of glucose depletion. In agreement with this hypothesis, δ_g
100 was inversely related to the initial cell density N_0, which modifies the rate of sugar
101 consumption (Supplementary Fig. 3B). In addition, a population that received a first step of
102 glucose and galactose, followed by an additional step input of glucose after 5 hours had a
103 significantly larger δ_g than a population that received only the initial dual-sugar input,
104 further corroborating the fact that δ_g is tuned by the concentration of glucose
105 (Supplementary Fig. 3C). In contrast to δ_g, $F_{ON\text{-}mid}$ was approximately equal in conditions
106 that received one or two steps of glucose, suggesting that the second glucose input did not
107 induce substantial switching between OFF and ON states (Supplementary Fig. 3D).
108
109 Our results indicate that galactose consumption did not commence for hours despite the
110 presence of a substantial subpopulation of GAL ON cells. Indeed, galactose consumption
111 did not initiate until approximately 85% of cells were activated (Fig. 2C and Supplementary
112 Fig. 4). Therefore, there is a broad regime where inhibition of galactose metabolism does
113 not require transcriptional repression of the GAL genes. In this region, the population

bioRxiv preprint doi: https://doi.org/10.1101/002907; this version posted February 21, 2014. The copyright holder for this preprint (which was not certified by peer review) is the author/funder, who has granted bioRxiv a license to display the preprint in perpetuity. It is made available under aCC-BY-NC-ND 4.0 International license.

114 adopts a previously undocumented bimodal regulatory strategy of activated and repressed
115 GAL states.
116
117 The absence of galactose metabolism does not result from decoupling galactose sensing
118 and trafficking. In this inducer exclusion model[14], extracellular galactose is sensed,
119 triggering GAL gene induction, but galactose does not permeate the cell due to glucose-
120 dependent inhibition of galactose transport. However, Gal1p and Gal3p are the only known
121 sensors of galactose and these proteins function intracellularly, indicating that a sufficient
122 amount of galactose was entering the cells to induce pathway activation[15]. Furthermore,
123 we observed a significant induction of pGAL2, accumulation of the fluorescently tagged
124 Gal2 permease in the activated subpopulation, localization of Gal2p-Venus to the
125 membrane in the presence of glucose and galactose and strong correlation between a Gal2
126 fluorescent protein fusion and pGAL10 in the presence of mixtures of glucose and galactose
127 (Supplementary Figs. 1 and 6).
128
129 To further rule out the possibility of inducer exclusion as an explanation of our findings, we
130 tested whether the level of Gal2p was limiting for the activation of the GAL pathway in the
131 presence of glucose. To do so, we used a TET inducible promoter to vary the concentration
132 of Gal2p in a strain deleted for the endogenous *GAL2* gene, and assessed the fraction of GAL
133 ON cells (as quantified using a pGAL10-Venus reporter) in response to simultaneous
134 addition of 0.5% galactose and a range of glucose levels (Supplementary Fig. 6D). We did
135 not observe any dependence of the fraction of ON cells on aTc concentration, and hence on

bioRxiv preprint doi: https://doi.org/10.1101/002907; this version posted February 21, 2014. The copyright holder for this preprint (which was not certified by peer review) is the author/funder, who has granted bioRxiv a license to display the preprint in perpetuity. It is made available under aCC-BY-NC-ND 4.0 International license.

136 Gal2p levels, suggesting that inducer exclusion does not dominate pathway activation in
137 the presence of glucose.
138
139 Taken together, our data suggest that in the cells where GAL genes are induced,
140 transcriptional and metabolic control seem to be decoupled. These results counter a central
141 premise of the Monod diauxic sugar model, predicated on the idea that expression of a
142 secondary sugar pathway is repressed in the presence of a preferred carbon source,
143 therefore blocking the utilization of the secondary sugar[4]. At the same time, our data are
144 consistent with the observation that the inhibition of galactose consumption in response to
145 a glucose pulse occurs on a timescale faster than can be explained by changes in
146 transcriptional regulation or protein degradation, therefore making it unlikely that the
147 catalytic degradation of Gal2p is the main effector of metabolic inhibition in the GAL
148 pathway[16].
149
150 To understand how the structure of the GAL regulatory network could generate the
151 observed transient bimodality in response to dual-sugar inputs, we constructed a
152 simplified mathematical model of this circuit based on canonical knowledge about the
153 galactose system (Supplementary Text)[17]. The GAL network has been shown to exhibit
154 memory of galactose and glucose exposure, suggesting bistability as the source bimodality
155 in this system[17,18]. In our model, the galactose input activates the signal transducer
156 Gal1p (G1) forming G1*, which inhibits the repressor Gal80p (G80) from sequestering the
157 transcriptional activator Gal4p (G4), thus leading to GAL gene activation (Fig. 3A). The
158 inhibition of G80 liberates G4 to induce expression of G1 and G80, establishing a positive

bioRxiv preprint doi: https://doi.org/10.1101/002907; this version posted February 21, 2014. The copyright holder for this preprint (which was not certified by peer review) is the author/funder, who has granted bioRxiv a license to display the preprint in perpetuity. It is made available under aCC-BY-NC-ND 4.0 International license.

159 and negative feedback loop. Since glucose has been shown to reduce the activity of the GAL
160 system, we coupled this model to an input of glucose[19]. We modeled GAL repression by
161 glucose assuming that a repressor R (such as Mig1), can be activated by the glucose signal
162 forming R*, which can then repress the promoters of *GAL1* and *GAL4*.
163
164 A salient qualitative feature of this mathematical model is that it can undergo a bifurcation
165 from monostability to bistability as a function of its two inputs: glucose and galactose (Fig.
166 3B). In response to low glucose and high-galactose inputs, the model exhibits one steady-
167 state, corresponding to the experimental ON state (high total G1 levels). For high glucose
168 and low galactose inputs, the only steady-state corresponds to the OFF state (low total G1
169 levels). Similar concentrations of the two inputs produce two stable steady-states that
170 correspond to the bimodality observed in the experiments.
171
172 This model also predicts the emergence and disappearance of bistability in the GAL system
173 as a function of time for a given dual sugar input. By assuming that the system traverses a
174 series of quasi-steady-states as a function of decaying sugar concentration (highlighted
175 panels in Fig. 1), a given model trajectory crosses through a region of bistability, which is
176 then transformed to monostability as glucose drops below a critical threshold (bifurcation
177 point) due to cellular consumption (representative trajectory in Fig. 3B). This transition
178 from bistable to monostable behavior at the glucose bifurcation point corresponds to the
179 synchronized delayed activation of the repressed cohort of cells. The observed monomodal
180 activation for sufficiently low glucose concentrations (left of highlighted panels in Fig. 1B)
181 and significantly delayed activation (right of highlighted panels in Fig. 1B) are also

bioRxiv preprint doi: https://doi.org/10.1101/002907; this version posted February 21, 2014. The copyright holder for this preprint (which was not certified by peer review) is the author/funder, who has granted bioRxiv a license to display the preprint in perpetuity. It is made available under aCC-BY-NC-ND 4.0 International license.

182 explained by the model (Supplementary Fig. 7). Furthermore, the model indicates that if
183 the glucose concentration were maintained above its value at the bifurcation point, for
184 example by replenishment of glucose (Supplementary Fig. 3C), then the window of time
185 where bistability exists in the system would be extended. This is precisely the case since
186 cultures that received an initial pulse of glucose and galactose followed by a second pulse
187 of glucose exhibited bimodality for a longer period of time compared to a culture that
188 received only the initial sugar mixture (Supplementary Fig. 3C).
189
190 In addition to explaining the origin of transient bimodality, the model made predictions
191 about different features of the system. First, the model had predictions about the role of
192 feedback loops. Removing the *GAL80* feedback loop in the model augmented the range of
193 glucose and galactose concentrations that produced bistability. This prediction was
194 qualitatively consistent with our data showing that the range of glucose and galactose
195 inputs that produced experimental bimodality was expanded in a strain lacking the Gal80p
196 feedback loop (Supplementary Fig. 8).
197
198 The bifurcation hypothesis provided by the model also implied that the amount of time
199 required for glucose to decrease to a threshold concentration corresponding to the
200 bifurcation point in the system (δ_b) should decrease if galactose is added at different times
201 following the glucose input (rather than concomitantly with glucose--for example, 0, 3.2,
202 3.5 3.7 or 3.9 hours following an initial glucose step) (Fig. 3C). This increasing delay in
203 galactose administration signifies a decreasing glucose concentration in the culture due to
204 cellular consumption at the time of galactose addition, and hence a reduced window of time

bioRxiv preprint doi: https://doi.org/10.1101/002907; this version posted February 21, 2014. The copyright holder for this preprint (which was not certified by peer review) is the author/funder, who has granted bioRxiv a license to display the preprint in perpetuity. It is made available under aCC-BY-NC-ND 4.0 International license.

205 for bistability. The delayed activation response corresponds to the loss of bistability as
206 glucose crosses a threshold bifurcation point. Hence δ_g and δ_b reflect similar properties of
207 the system.
208
209 To experimentally test this prediction, we applied a step input of 0.1% galactose at
210 different times to a set of cultures that had all received 0.1% glucose from time zero. In
211 condition A, both sugars were added simultaneously at time zero, while in cultures B-E,
212 galactose was added 3.1, 4.2, 5.3 and 6.3 hours following the glucose stimulus (arrows in
213 Fig. 3D). Matching the trend of decreasing δ_b in the model (Fig. 3C), bimodality emerged at
214 the time of the galactose input and δ_g contracted and eventually disappeared with the
215 increased delay in this input (right panel in Fig. 3D, Supplementary Fig. 9).
216
217 Finally, the model indicated that the response time of the system to transition from the OFF
218 to the ON state decreases as glucose decays. The system's response time is dictated by both
219 the domain of attraction and the magnitude of the dominant eigenvalue of the ON steady-
220 state (Supplementary Text), which both increase as glucose decreases (Fig. 3E). Therefore,
221 the model predicts that the response time of the fraction of ON cells should decrease in the
222 delayed galactose experiment. Corroborating this insight, our experimental data
223 demonstrated a decrease in the response time of F_{ON} with an increase in the delay of the
224 galactose input (Fig. 3F,G). Therefore, in addition to providing a framework that explains
225 the transition of the GAL system between different phenotypic modes, our model and its
226 validated predictions demonstrate the intricate modulation of quantitative properties of
227 this network by its environmental inputs. As we discuss below, this constitutes an

bioRxiv preprint doi: https://doi.org/10.1101/002907; this version posted February 21, 2014. The copyright holder for this preprint (which was not certified by peer review) is the author/funder, who has granted bioRxiv a license to display the preprint in perpetuity. It is made available under aCC-BY-NC-ND 4.0 International license.

228 important feature that distinguishes this strategy from previously documented
229 stochastically dominated bet-hedging mechanisms.
230
231 We next probed the physiological impact of the observed anticipatory induction of the GAL
232 regulatory program hours in advance of galactose consumption by analyzing the
233 relationship between the timing of GAL pathway activation and the population's growth
234 rate and metabolism. To do so, we quantified the concentrations of glucose, galactose and
235 growth rates for the different cultures that were subjected to delayed galactose inputs over
236 time in the experiment described above. Irrespective of galactose timing, glucose decayed
237 at a similar rate for all conditions (Fig. 4A). Despite the presence of glucose at the time of
238 the galactose stimulus for conditions A-D, galactose consumption was delayed compared to
239 the culture that received glucose and galactose simultaneously (Fig. 4B,C). Furthermore,
240 the delay in galactose consumption was increased commensurately with the delay in
241 galactose administration. Notably, during the metabolic shift between carbon sources, the
242 population that received galactose simultaneously with glucose exhibited a transient
243 growth rate advantage, reaching approximately 25% compared to the population that
244 received this sugar after a 6.3-hour delay (E) (Fig. 4D, Supplementary Fig. 10). Since the
245 growth rate is proportional to the current size of the population in exponential phase, the
246 significance of this fitness difference increases with each cell generation. Overall, the delay
247 in galactose input caused a monotonic increase in the transient growth defect, which was
248 manifested as an increase in the "lag" time between the two phases of growth documented
249 by Monod (Supplementary Fig. 10A)[4]. Importantly, the presence of galactose did not
250 benefit the population of cells until total glucose depletion (Fig. 4D inset, Supplementary

bioRxiv preprint doi: https://doi.org/10.1101/002907; this version posted February 21, 2014. The copyright holder for this preprint (which was not certified by peer review) is the author/funder, who has granted bioRxiv a license to display the preprint in perpetuity. It is made available under aCC-BY-NC-ND 4.0 International license.

251 Figs. 10A and 11, Supplementary Text). Taken together, these data indicate that the
252 induction of the GAL pathway many cell generations before these genes are required
253 provides a transient fitness advantage during the shift between carbon sources.
254
255 This beneficial pre-emptive induction of the GAL pathway genes only occurs in a subset of
256 the population. To investigate the tradeoffs that might motivate this bimodal induction,
257 versus a uniform strategy in which all the cells in the population pre-emptively but
258 coherently induce the GAL pathway, we sought to control GAL gene expression
259 independently of galactose. To do so, we used an estradiol inducible Gal4 chimera in a
260 strain lacking endogenous Gal4p[20,21]. In this strain, we could activate GAL gene
261 expression on demand at specific times before glucose depletion in cultures subjected to
262 0.1% glucose and 0.1% galactose from time zero (Supplementary Fig. 12A).
263
264 Since the synthetic inducible system is not connected to the feedback structure of the
265 natural circuit, GAL gene expression was monomodal (graded) as opposed to bimodal in
266 this strain. In this case, early activation of the GAL pathway generated a lower consumption
267 rate of glucose compared to late activation, demonstrating that constitutive GAL gene
268 expression can inhibit glucose consumption (Supplementary Fig. 12B). The expression
269 level of pGAL10 induced by this synthetic system was very similar to the expression level of
270 pGAL10 in the wild type (Supplementary Fig. 13A). Therefore, the effects we observed are
271 not likely to be a consequence of over or under expression of the GAL genes. Constitutive
272 induction of the GAL pathway through over expression of Gal3p also reduced the glucose
273 consumption rate (Supplementary Fig. 13, Supplementary Text). Together, these data

bioRxiv preprint doi: https://doi.org/10.1101/002907; this version posted February 21, 2014. The copyright holder for this preprint (which was not certified by peer review) is the author/funder, who has granted bioRxiv a license to display the preprint in perpetuity. It is made available under aCC-BY-NC-ND 4.0 International license.

274 highlight an important tradeoff that the system has to balance: induction of the GAL genes
275 before they are required results in faster galactose consumption upon glucose depletion,
276 facilitating the transition between carbon substrates. At the same time, wholesale induction
277 of these genes across the entire population comes at the cost of a reduced rate of glucose
278 consumption. In agreement with this observation, the repressed subpopulation had
279 approximately 20% faster growth rate on average than that of the activated subpopulation
280 in the transient bimodal region in the wild type (Supplementary Fig. 14, Supplementary
281 Text). However, in this bimodal regime, the glucose consumption rate of the whole
282 population was not saliently reduced by GAL gene expression in a subpopulation of cells
283 (Fig. 4A). Therefore, the bimodal strategy seems to be efficiently balancing the tradeoffs
284 imposed by the pre-emptive induction of the galactose transcriptional program.
285

286 **DISCUSSION**

287 In this work, we demonstrate that a combinatorial input of glucose and galactose triggers
288 diverse regulatory states across a population of cells. This transient bimodality establishes
289 the co-existence of two subpopulation of cells--one that prepares hours in advance for a
290 future shift in carbon metabolism and a second that defers pathway activation over many
291 cell generations until these genes are required. The fraction of cells that occupy each state
292 is tuned by the dual-sugar mixture, standing in contrast to canonical models in which the
293 output of a pathway is proportionally matched to the level of its inputs in all cells of the
294 population[22,23]. This mechanism also seems to be an elaboration on bet-hedging
295 processes where stochastic fluctuations diversify the phenotypic states of a population in
296 the absence of an environmental trigger[7,13,24], although in some instances,

bioRxiv preprint doi: https://doi.org/10.1101/002907; this version posted February 21, 2014. The copyright holder for this preprint (which was not certified by peer review) is the author/funder, who has granted bioRxiv a license to display the preprint in perpetuity. It is made available under aCC-BY-NC-ND 4.0 International license.

297 environmental cues have been implicated in biasing the distribution of phenotypic
298 states[25,26]. There are some examples of biological networks that seem to have evolved
299 the ability to activate multiple distinct signaling pathways simultaneously in response to a
300 single environmental input as a consequence of temporal correlations between different
301 environmental signals[27,28]. The strategy we describe is also unique in that the response
302 of the GAL system integrates direct environmental sensing with pre-emption of a future
303 metabolic shift.
304
305 Although our data do not pinpoint the exact mechanism by which glucose inhibits the
306 metabolism of galactose in GAL ON cells, previous studies hint that this inhibition might be
307 mediated by the dominant glucose kinase Hxk2p. Indeed, glucose and galactose are
308 consumed simultaneously in cells lacking Hxk2p[29]. Furthermore, in *S. cerevisiae*, glucose
309 was shown to block the maltose pathway (MAL) by a novel mechanism at the signaling
310 level, which is also linked to Hxk2p[30] and distinct from inducer exclusion. It is therefore
311 possible that the GAL and MAL pathways share similar post-translational inhibitory
312 mechanisms by glucose.
313
314 Our data reveal that the induction of the GAL pathway in a fraction of the *S. cerevisiae*
315 population before depletion of its preferred sugar (glucose) provides a kinetic advantage
316 by shortening the lag phase before growth can resume on the secondary sugar.
317 Evolutionary tuning of the duration of the lag phase has been shown to be a crucial variable
318 for fitness of microbial populations in fluctuating environments[31]. Therefore, it is
319 tempting to speculate that the advantage we characterize may be substantial for cells facing

bioRxiv preprint doi: https://doi.org/10.1101/002907; this version posted February 21, 2014. The copyright holder for this preprint (which was not certified by peer review) is the author/funder, who has granted bioRxiv a license to display the preprint in perpetuity. It is made available under aCC-BY-NC-ND 4.0 International license.

320 competition from other species for limited resources[32,33]. In agreement with this
321 hypothesis, heterogeneity in the expression of the Lac operon in *E. coli* has recently been
322 shown to modify the growth rates of single cells during the transition from glucose to
323 lactose metabolism[34]. Furthermore, combinatorial carbon sources have been shown to
324 trigger genetic mutations that produce phenotypic population diversification in *E. coli*[35].
325 Future studies that probe the broad adoption of similar strategies in other microorganisms,
326 including *S. cerevisiae,* may yield insights into the precise evolutionary advantages of this
327 response, and explore its use as a general paradigm for survival and reproduction in
328 complex competitive environments.

bioRxiv preprint doi: https://doi.org/10.1101/002907; this version posted February 21, 2014. The copyright holder for this preprint (which was not certified by peer review) is the author/funder, who has granted bioRxiv a license to display the preprint in perpetuity. It is made available under aCC-BY-NC-ND 4.0 International license.

329 **MATERIALS AND METHODS**

330 Growth conditions and flow cytometry

331 Cells were grown in yeast peptone media for approximately 12 hours and then diluted to
332 an optical density (OD) of approximately 0.3 prior to induction with glucose and galactose.
333 Single-cell fluorescence was measured on a LSRII analyzer (BD Biosciences). A blue (488
334 nm) laser was used to excite YFP and emission was detected using a 530/30 nm filter.
335 1000-20,000 cells were collected for each dynamic measurement.
336

337 Automated flow cytometry measurements

338 A 500 μl culture volume was used in 96-well plate format for the automated flow cytometry
339 measurements as described in ref. 9. For each time point, a 30 μl sample was removed from
340 the culture for measurement on the cytometer and 30 μl of fresh media containing the
341 appropriate 1X concentration of glucose and galactose was used as replacement to
342 maintain a constant culture volume.
343

344 Flask measurements

345 A 60 ml culture volume was used for the flask experiments in which the sugar
346 concentrations were quantified. Less than 5% of the total volume was removed over the
347 course of the experiment to quantify the single cell fluorescence, sugar concentrations and
348 absorbance at 600 nm (OD). OD was measured on a Nanodrop 2000c spectrophotometer
349 (Thermo Scientific).
350

351 Quantitative analysis of gene expression dynamics

bioRxiv preprint doi: https://doi.org/10.1101/002907; this version posted February 21, 2014. The copyright holder for this preprint (which was not certified by peer review) is the author/funder, who has granted bioRxiv a license to display the preprint in perpetuity. It is made available under aCC-BY-NC-ND 4.0 International license.

352 The ratio of YFP fluorescence to side scatter was used to quantify the total fluorescence per
353 cell. Flow cytometry distributions were analyzed using a Gaussian mixture model algorithm
354 (GMM, MATLAB) and each distribution was classified as either unimodal or bimodal as
355 described in ref. 19. The delay time δ_a was computed as the time required to reach the half-
356 max of the mean of the activated subpopulation. δ_g was defined as the difference between
357 the time required to reach the half-max of the mean of the activated and repressed
358 subpopulations. The fraction of ON cells (F_{ON}) was computed as the fraction of the cell
359 population higher than a fluorescence threshold ($10^{-0.2}$ a.u.) that corresponds to
360 approximately the lowest density of single-cell fluorescence between the OFF and ON
361 expression states. $F_{ON\text{-}mid}$ was quantified at the midpoint between the half-max of the
362 activated (δ_a) and repressed subpopulations. The response time was defined as the time to
363 reach the half-max of F_{ON} (F_{ON} = 0.5). At each time point, individual cells were assigned to
364 the OFF and ON states using the F_{ON} threshold on gene expression described above. The
365 subpopulation growth rates were computed as the slope of a line fit to the $\log_2$ of the
366 number of cells that accumulated in the OFF and ON states over time.
367
368 Sugar measurements
369 Glucose and galactose were measured using the Amplex Red glucose oxidase and galactose
370 oxidase kits (Molecular Probes, Life Technologies). A Tecan Safire plate reader (Tecan) was
371 used to quantify the fluorescence. A standard of known concentration for each sugar was
372 used to determine the quantitative relationship between the fluorescence and sugar
373 concentration.
374

bioRxiv preprint doi: https://doi.org/10.1101/002907; this version posted February 21, 2014. The copyright holder for this preprint (which was not certified by peer review) is the author/funder, who has granted bioRxiv a license to display the preprint in perpetuity. It is made available under aCC-BY-NC-ND 4.0 International license.

375 Microscopy measurements

376 Cells were attached to glass-bottom wells in a 96-well plate (Matrical) functionalized with
377 concanavalin-A (Sigma). Fluorescence images were taken at room temperature on a Nikon
378 Ti-E equipped with a Perfect Focus System and a Coolsnap HQ2 CCD camera
379 (Photometrics).

380

381 Computational modeling

382 We used custom made code for mathematical modeling written in MATLAB (Mathworks)
383 and Mathematica (Wolfram Research). Details about the model construction are provided
384 in the Supplementary Text. The domain of attraction of the ON steady state was defined as
385 the fraction of initial conditions that were assimilated by the ON equilibrium point and was
386 determined by randomly sampling 5000 initial conditions using the Latin Hypercube
387 Method[17]. A minimum and maximum bound on the concentration of each species was
388 used based on the parameters of the model. The dominant eigenvalue was defined as the
389 eigenvalue of smallest absolute value of the linearization at the ON equilibrium point.

bioRxiv preprint doi: https://doi.org/10.1101/002907; this version posted February 21, 2014. The copyright holder for this preprint (which was not certified by peer review) is the author/funder, who has granted bioRxiv a license to display the preprint in perpetuity. It is made available under aCC-BY-NC-ND 4.0 International license.

REFERENCES

1. Perkins TJ, Swain PS (2009) Strategies for cellular decision-making. Mol Syst Biol 5: 326.

2. Dienert F (1899) Sur la fermentation du galactose. Comptes Rendus Hebd des Seances l'Academie des Sci Paris 128: 569–571.

3. Dienert F (1900) Sur la fermentation du galactose et sur l'accoutumance des levures a ce sucre. Ann Inst Pasteur (Paris) 14: 139–189.

4. Monod J (1942) Recherches sur la croissance des cultures bacteriennes (Studies on the growth of bacterial cultures). Actual Sci Ind 911: 1–215.

5. Monod J (1949) The growth of bacterial cultures. Annu Rev Microbiol 3: 371–394.

6. Magasanik B (1970) The Lactose Operon. Cold Spring Harbor, NY: Cold Spring Harbor Laboratory Press.

7. Losick R, Desplan C (2008) Stochasticity and cell fate. Science (80-) 320: 65–68.

8. Zuleta, I. A., Aranda-diaz, A., Li., H., El-Samad H (2013) Dynamic characterization of gene expression and growth using automated high-throughput flow cytometry. Submitted.

9. Entian KD, Barnett JA (1992) Regulation of sugar utilization in Saccharomyces cerevisiae. Trends Biochem Sci 17: 506–510.

10. Gancedo JM (1998) Yeast carbon catabolite repression. Microbiol Mol Biol Rev 62: 334–361.

11. Kaufmann BB, Yang Q, Mettetal JT, van Oudenaarden A (2007) Heritable stochastic switching revealed by single-cell genealogy. PLoS Biol 5: e239.

12. Kepler TB, Elston TC (2001) Stochasticity in transcriptional regulation: origins, consequences and mathematical representations . Biophys J 81: 3116–3136.

13. Srikantha T, Zhao R, Daniels K, Radke J, Soll DR (2005) Phenotypic Switching in Candida glabrata Accompanied by Changes in Expression of Genes with Deduced Functions in Copper Detoxification and Stress. Eukaryot Cell 4: 1434–1445.

14. Gorke B, Stulke J (2008) Carbon catabolite repression in bacteria: many ways to make the most out of nutrients. Nat Rev Microbiol 6: 613–624.

bioRxiv preprint doi: https://doi.org/10.1101/002907; this version posted February 21, 2014. The copyright holder for this preprint (which was not certified by peer review) is the author/funder, who has granted bioRxiv a license to display the preprint in perpetuity. It is made available under aCC-BY-NC-ND 4.0 International license.

15. Torchia TE, Hopper JE (1986) Genetic and molecular analysis of the GAL3 gene in the expression of the galactose/melibiose regulon of Saccharomyces cerevisiae. Genetics 113: 229–246.

16. Sierkstra LN, Nouwen NP, Verbakel JM, Verrips CT (1992) Analysis of glucose repression in Saccharomyces cerevisiae by pulsing glucose to a galactose-limited continuous culture. Yeast 8: 1077–1087.

17. Venturelli OS, El-Samad H, Murray RM (2012) Synergistic dual positive feedback loops established by molecular sequestration generate robust bimodal response. Proc Natl Acad Sci 109.

18. Zacharloudakis I, Gligoris T, Tzamarias D (2007) A yeast catabolic enzyme controls transcriptional memory. Curr Biol 17: 2041–2046.

19. Johnston M, Flick JS, Pexton T (1994) Multiple mechanisms provide rapid and stringent glucose repression of GAL gene expression in Saccharomyces cerevisiae. Mol Cell Biol 14: 3834–3841.

20. Louvion JF, Havaux-Copf B, Picard D (1993) Fusion of GAL4-VP16 to a steroid-binding domain provides a tool for gratuitous induction of galactose-responsive genes in yeast. Gene 131: 129–134.

21. Stewart-Ornstein J, Weissman JS, El-Samad H (2012) Cellular Noise Regulons Underlie Fluctuations in Saccharomyces cerevisiae. Mol Cell 45: 483–493.

22. Pincus D, Chevalier MW, Aragon T, van Anken E, Vidal SE, et al. (2010) BiP binding to the ER-stress sensor Ire1 tunes the homeostatic behavior of the unfolded protein response. PLoS Biol 8: e1000415.

23. Dekel E, Alon U (2005) Optimality and evolutionary tuning of the expression level of a protein. Nature 436: 588–592.

24. Balaban NQ, Merrin J, Chait R, Kowalik L, Leibler S (2004) Bacterial persistence as a phenotypic switch. Science (80-) 305: 1622–1625.

25. Olsen PB, Schembri M a, Gally DL, Klemm P (1998) Differential temperature modulation by H-NS of the fimB and fimE recombinase genes which control the orientation of the type 1 fimbrial phase switch. FEMS Microbiol Lett 162: 17–23.

26. Grodzicker T, Arditti RR, Eisen H (1972) Establishment of repression by lambdoid phage in catabolite activator protein and adenylate cyclase mutants of Escherichia coli. Proc Natl Acad Sci U S A 69: 366–370.

27. Tagkopoulos I, Liu Y-C, Tavazoie S (2008) Predictive behavior within microbial genetic networks. Science (80-) 320: 1313–1317.

bioRxiv preprint doi: https://doi.org/10.1101/002907; this version posted February 21, 2014. The copyright holder for this preprint (which was not certified by peer review) is the author/funder, who has granted bioRxiv a license to display the preprint in perpetuity. It is made available under aCC-BY-NC-ND 4.0 International license.

28. Mitchell A, Romano GH, Groisman B, Yona A, Dekel E, et al. (2009) Adaptive prediction of environmental changes by microorganisms. Nature 460: 220–224.

29. Raamsdonk LM, Diderich JA, Kuiper A, van Gaalen M, Kruckeberg AL, et al. (2001) Co-consumption of sugars or ethanol and glucose in a Saccharomyces cerevisiae strain deleted in the HXK2 gene. Yeast 18: 1023–1033.

30. Hu Z, Yue Y, Jiang H, Zhang B, Sherwood PW, et al. (2000) Analysis of the mechanism by which glucose inhibits maltose induction of MAL gene expression in Saccharomyces. Genetics 154: 121–132.

31. Travisano M, Lenski RE (2013) Long-term experimental evolution in Escherichia coli. Changes in life history traits during adaptation to a seasonal environment. Am Nat 144: 432–456.

32. MacLean RC (2008) The tragedy of the commons in microbial populations: insights from theoretical, comparative and experimental studies. Heredity (Edinb) 100: 233–239.

33. Pfeiffer T, Schuster S, Bonhoeffer S (2001) Cooperation and competition in the evolution of ATP-producing pathways. Science (80-) 292: 504–507.

34. Boulineau S, Tostevin F, Kiviet DJ, ten Wolde PR, Nghe P, et al. (2013) Single-cell dynamics reveals sustained growth during diauxic shifts. PLoS One 8: e61686.

35. Friesen ML, Saxer G, Travisano M, Doebeli M (2004) Experimental evidence for sympatric ecological diversification due to frequency-dependent competition in Escherichia coli. Evolution 58: 245–260.

ACKNOWLEDGEMENTS
We would like to thank Adam Rosenthal and Michael Chevalier for helpful discussions and Carol Gross, Sandy Johnson, and Zev Gartner for critical reading of this manuscript. This research was supported by the Institute for Collaborative Biotechnologies through grant W911NF-09-0001 from the U.S. Army Research Office to R.M.M., the NIGMS system biology center (P50 GM081879) to H.E.S., and the David and Lucille Packard Foundation to H.E.S.

AUTHOR CONTRIBUTIONS
All authors designed the experiments. O.V. and I.Z. carried out the experiments. O.V. performed the computational modeling and analyzed the data. All authors contributed to data interpretation and writing of the manuscript.

bioRxiv preprint doi: https://doi.org/10.1101/002907; this version posted February 21, 2014. The copyright holder for this preprint (which was not certified by peer review) is the author/funder, who has granted bioRxiv a license to display the preprint in perpetuity. It is made available under aCC-BY-NC-ND 4.0 International license.

FIGURE LEGENDS

Figure 1

Dynamic responses of the GAL pathway to combinatorial inputs of glucose and galactose. (A) Single cell fluorescence distributions of pGAL10-Venus as a function of time in wild type *S. cerevisiae* obtained using automated flow cytometry for a wide range of glucose and galactose concentrations. In each subplot, the x-axis is time and the y-axis is fluorescence. Dashed box indicates the condition shown in panel **B** and highlighted conditions were used to quantify the duration of bimodality (δ_g) in panel **D. (B)** Fluorescent microscopy image of pGAL10-Venus induced simultaneously with 0.25% glucose and 0.5% galactose at time zero and measured after 6 hours (top, corresponds to dashed box in panel **A**). pGAL10-Venus flow cytometry distributions as a function of time highlighting transient bimodality (bottom). δ_a represents the response time of the early activated subpopulation, δ_g represents the duration of bimodality for quantifiable conditions in panel **A** (highlighted conditions) and $F_{ON\text{-}mid}$ denotes the fraction of cells in the ON state at the midpoint of the transient bimodal region (16). **(C)** Relationship between initial glucose levels and δ_a for a range of initial galactose concentrations. **(D)** Relationship between initial glucose concentrations and δ_g for different initial galactose levels. **(E)** Relationship between initial galactose levels and $F_{ON\text{-}mid}$ for different initial concentrations of glucose.

Figure 2

Glucose is consumed before galactose despite the presence of a subpopulation of cells with an active GAL pathway. Wild type cells were exposed to 0.1% glucose and 0.1% galactose simultaneously at time zero. **(A)** Representative dynamic measurements of glucose, galactose and the fraction of ON cells (F_{ON}) for wild type expressing p*GAL10*-Venus. Highlighted box indicates plateaued region. Lines represent fitted Hill functions. **(B)** Scatter plot of glucose concentrations and F_{ON} for the *GAL1*, *GAL2*, *GAL7* and *GAL10* promoter fusions to Venus measured over time. **(C)** Scatter plot of galactose concentrations and F_{ON} for p*GAL1*, p*GAL2*, p*GAL7* and p*GAL10*.

Figure 3

Computational model of GAL system with glucose and galactose inputs explains the origin of transient bimodality and predicts the dependence of the system on its inputs. (A) Schematic diagram of GAL circuit. Glu represents glucose and gal represents galactose. The activated molecules are represented by R* and G1*. Pointed and blunted arrows indicate activation and repression, respectively. **(B)** Bifurcation diagram at steady-state. Bistability is represented by white and colored regions denote monostability. Total concentration of G1 is denoted by $G1_T$. Time zero is indicated by t_0 and solid lines highlight a model trajectory of sequential consumption of the two sugars by a cell population. **(C)** Bifurcation diagram at steady-state (left). Arrows denote the addition of galactose at different times to a system that received glucose at t_0. δ_b is computed as the time required for glucose to decay to the bifurcation point threshold (right). **(D)** Mean expression levels of ON and OFF subpopulations for the delayed galactose experiment (left) and duration of bimodality (δ_g) (right). Arrows indicate the time of the galactose stimulus. **(E)** The fraction

bioRxiv preprint doi: https://doi.org/10.1101/002907; this version posted February 21, 2014. The copyright holder for this preprint (which was not certified by peer review) is the author/funder, who has granted bioRxiv a license to display the preprint in perpetuity. It is made available under aCC-BY-NC-ND 4.0 International license.

of initial conditions (IC) and the dominant eigenvalue for the ON equilibrium state as a function of glucose for 150 nM galactose. **(F)** Experimental measurements of F_{ON} in the galactose step experiment over time. Response time of F_{ON} for each condition (right). Error bars indicate one s.d. from the mean of two replicates.

Figure 4
Early GAL pathway induction establishes a growth advantage during carbon source switch. Measurements of glucose, galactose and growth rates for delayed galactose experiment in which 0.1% galactose was added to a set of cultures at different times that had all received 0.1% glucose from time zero. Arrows indicate the time of the galactose stimulus. **(A)** Glucose concentrations as a function of time for each condition. **(B)** Galactose concentrations as a function of time for each condition. Lines represent fitted Hill functions. **(C)** Fractional change in the half-max of the galactose decay curves for each condition relative to condition A. **(D)** Normalized growth rates of conditions B-F compared to A (red line). Un-normalized growth rates for each condition (inset). Error bars represent one s.d. from the mean of two replicates.

bioRxiv preprint doi: https://doi.org/10.1101/002907; this version posted February 21, 2014. The copyright holder for this preprint (which was not certified by peer review) is the author/funder, who has granted bioRxiv a license to display the preprint in perpetuity. It is made available under aCC-BY-NC-ND 4.0 International license.

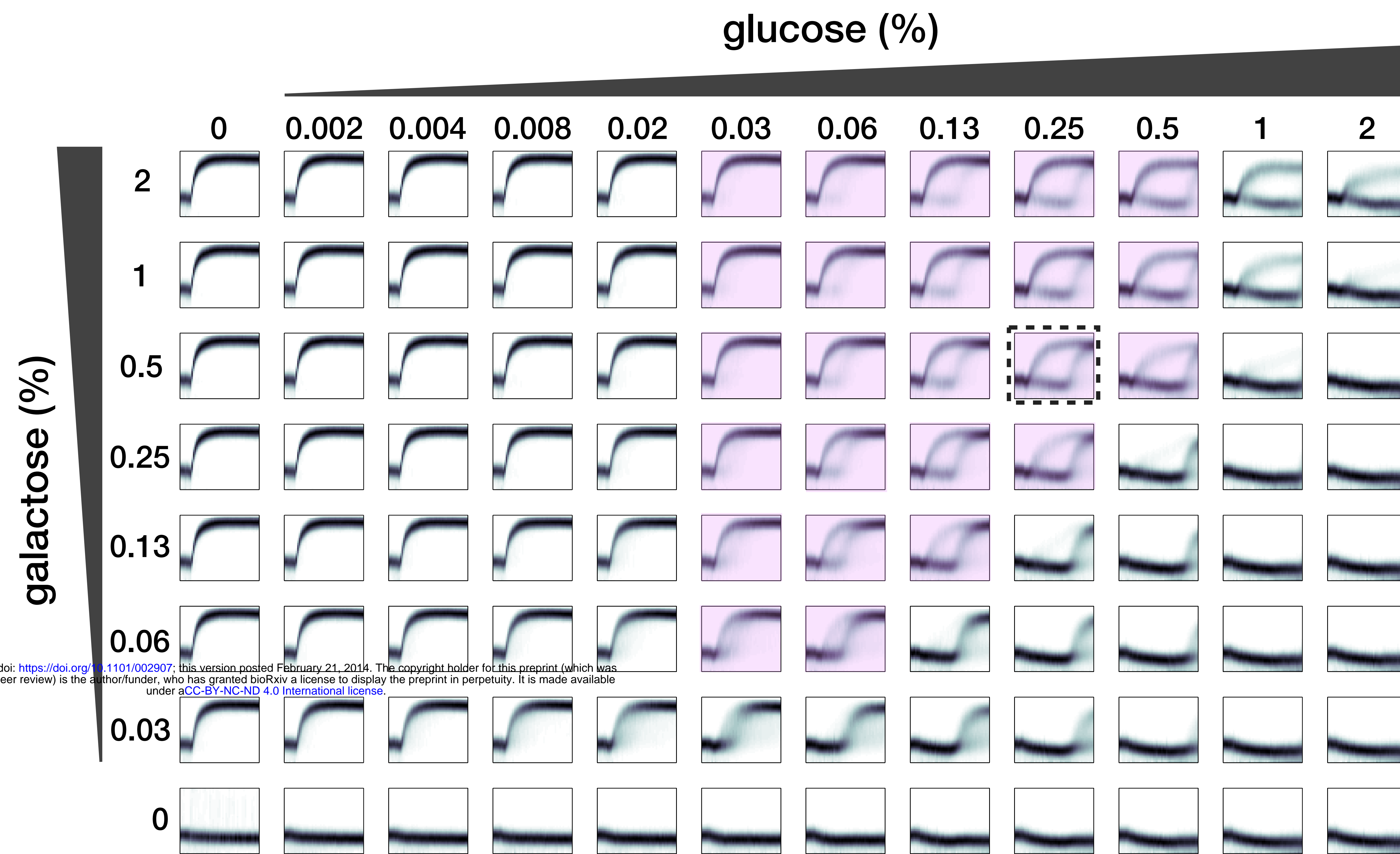

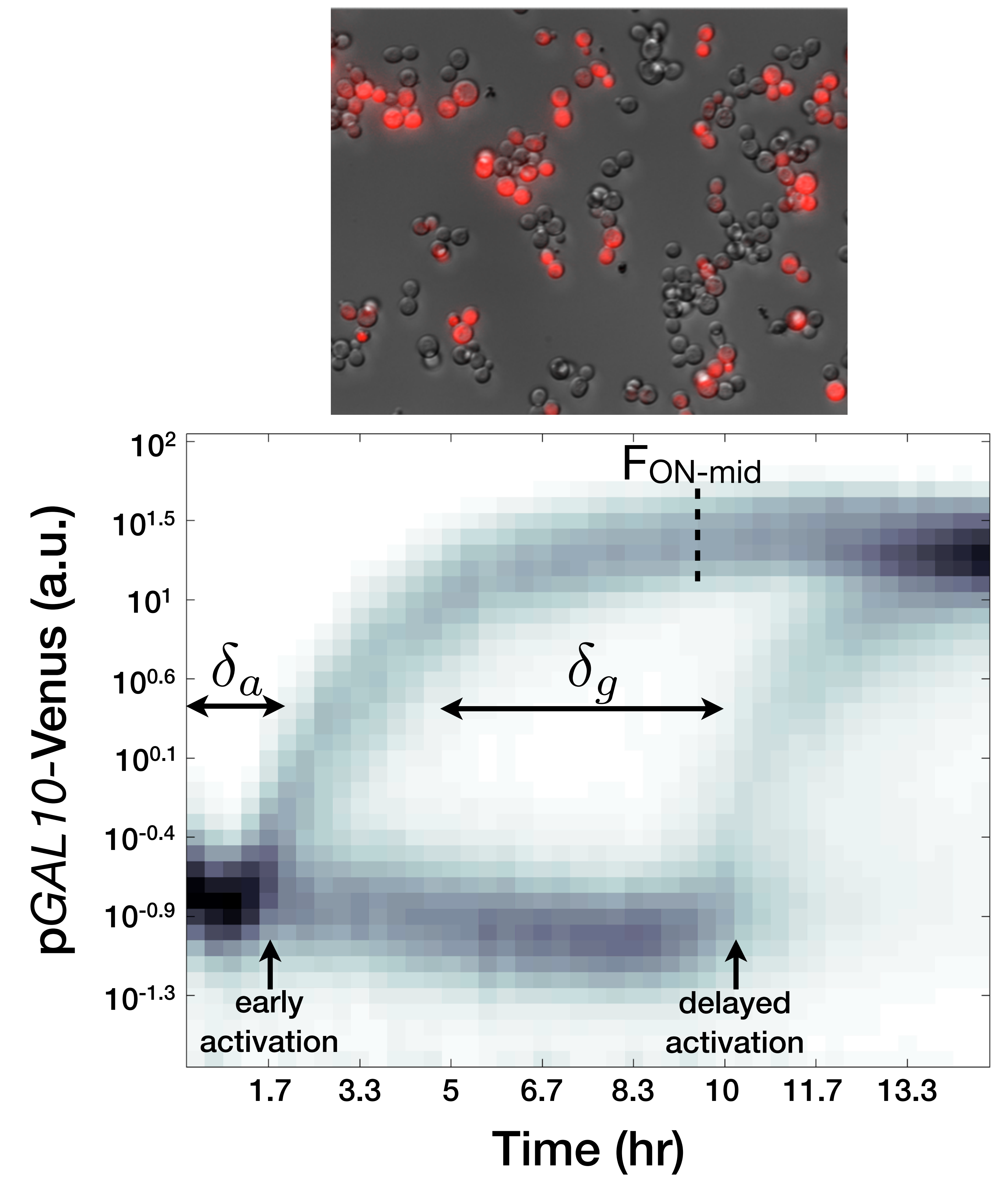

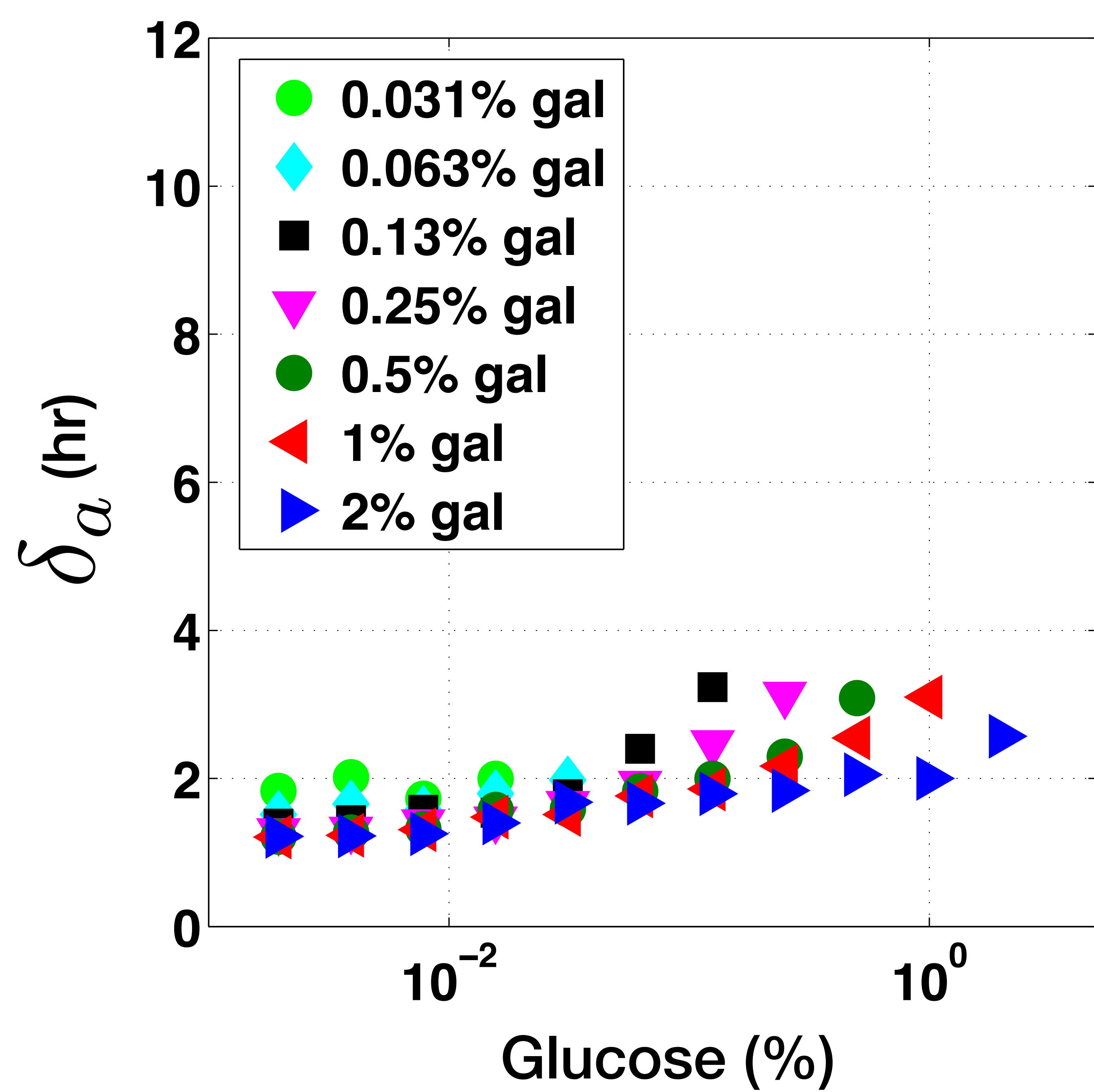

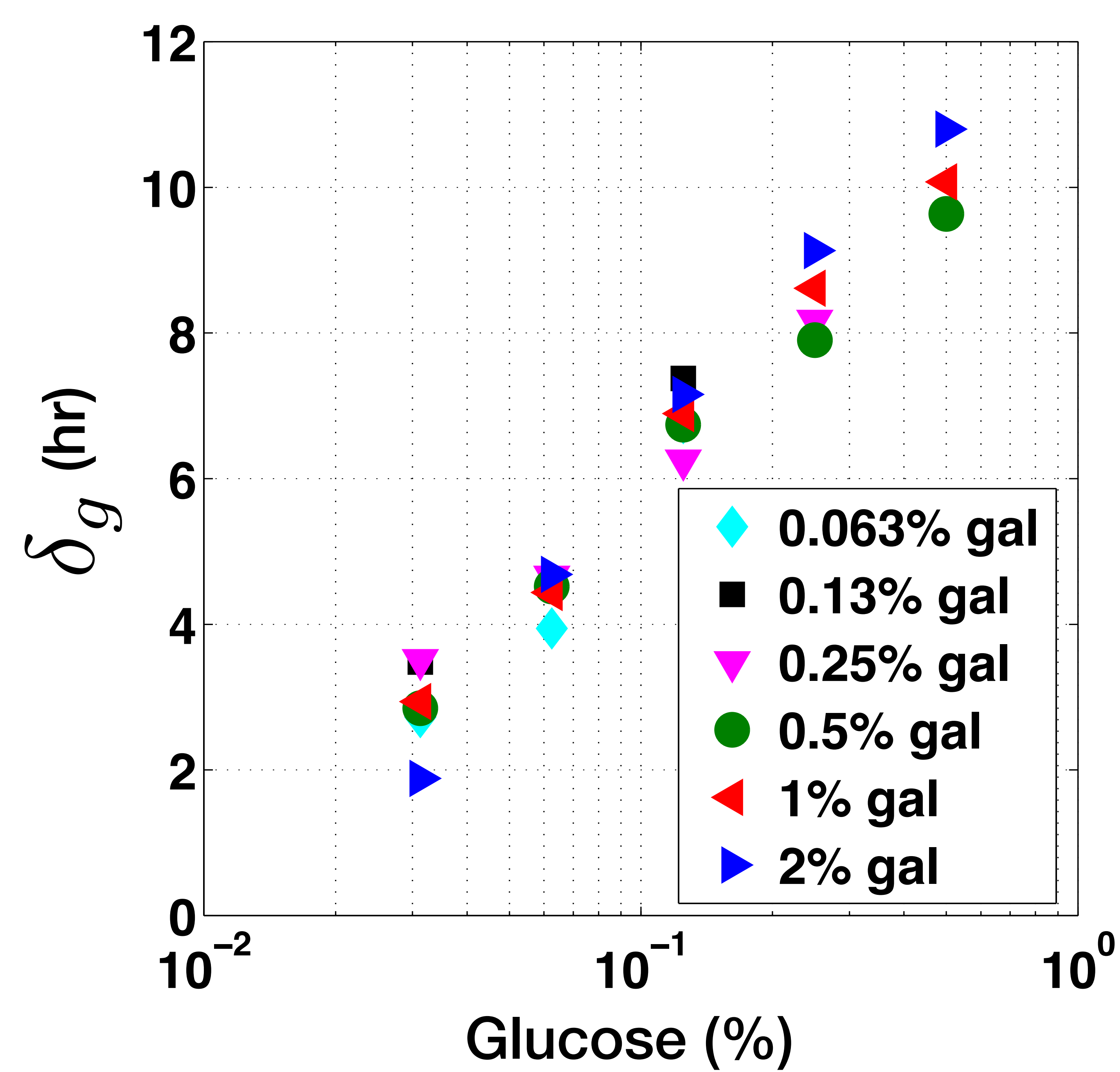

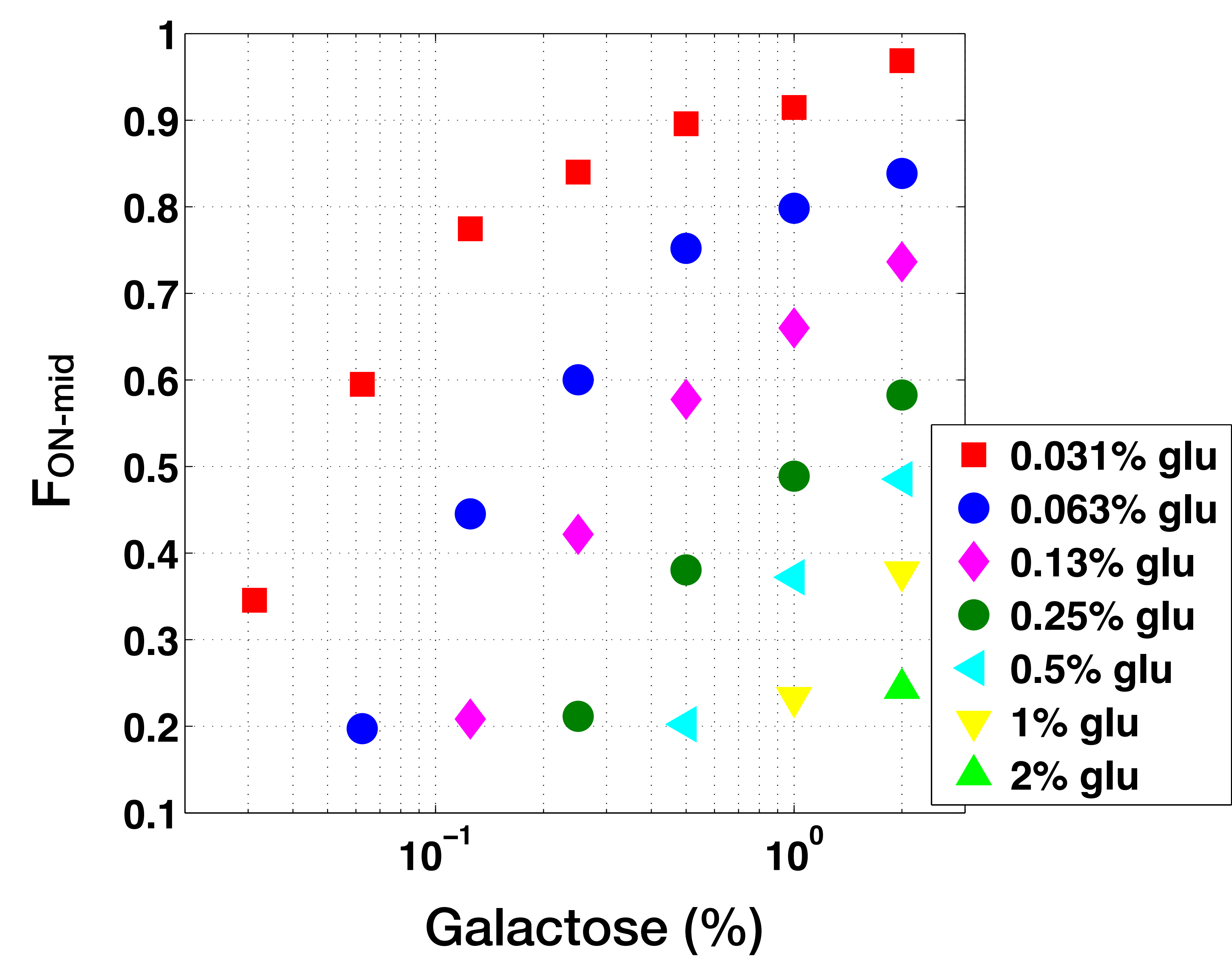

not certified by peer review) is the author/funder, who has granted bioRxiv a license to display the preprint in perpetuity. It is made available under aCC-BY-NC-ND 4.0 International license.

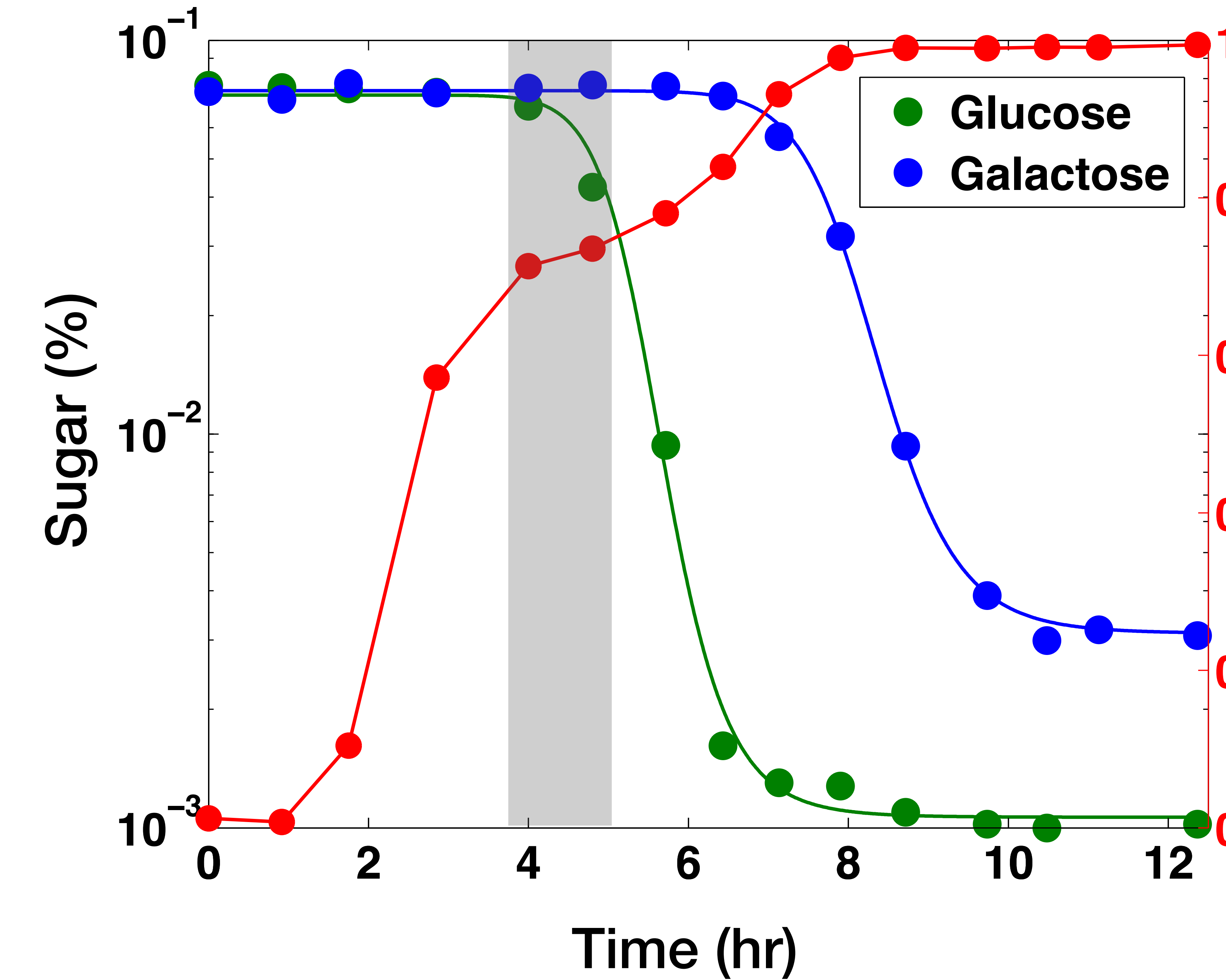

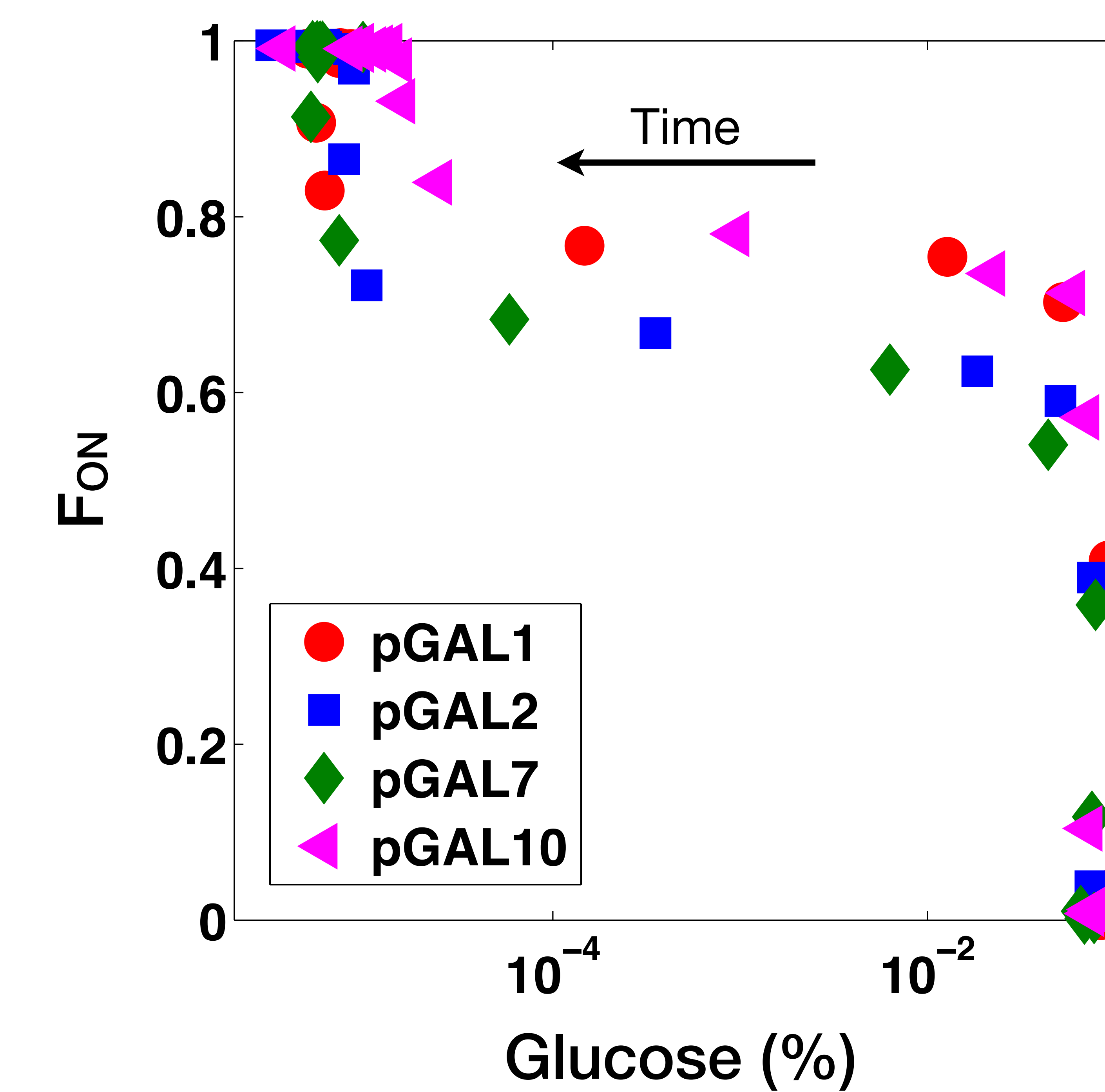

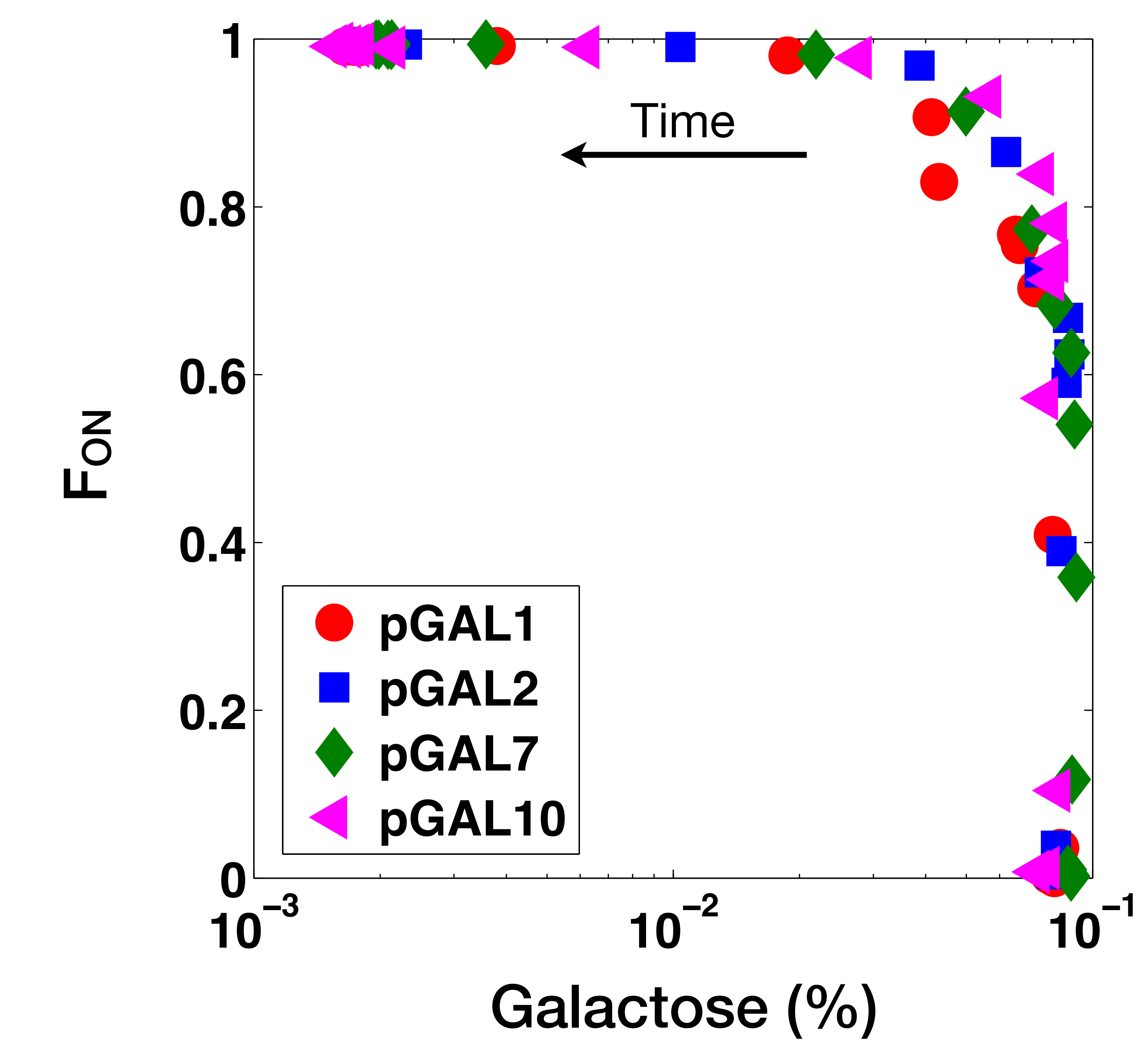

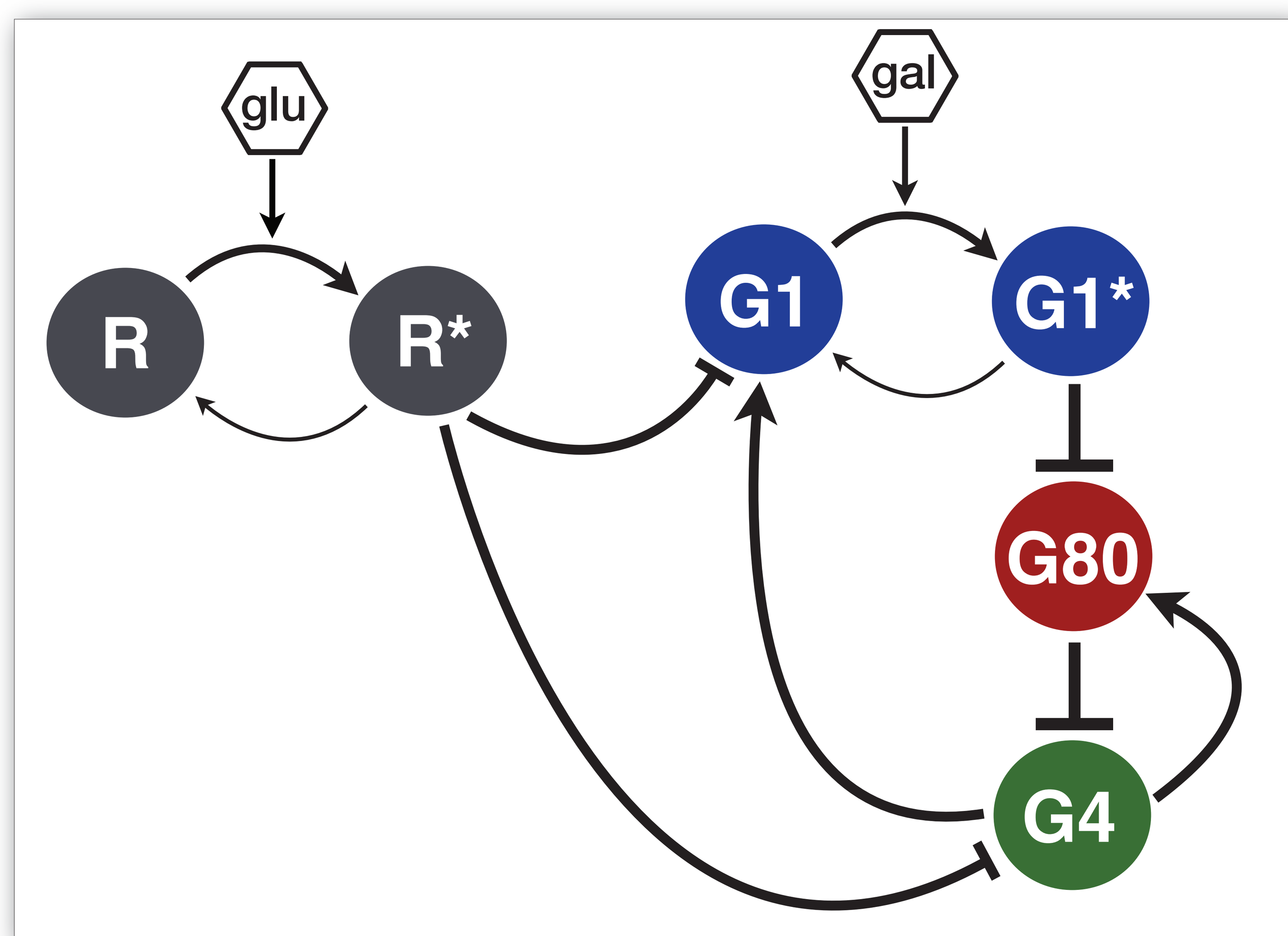

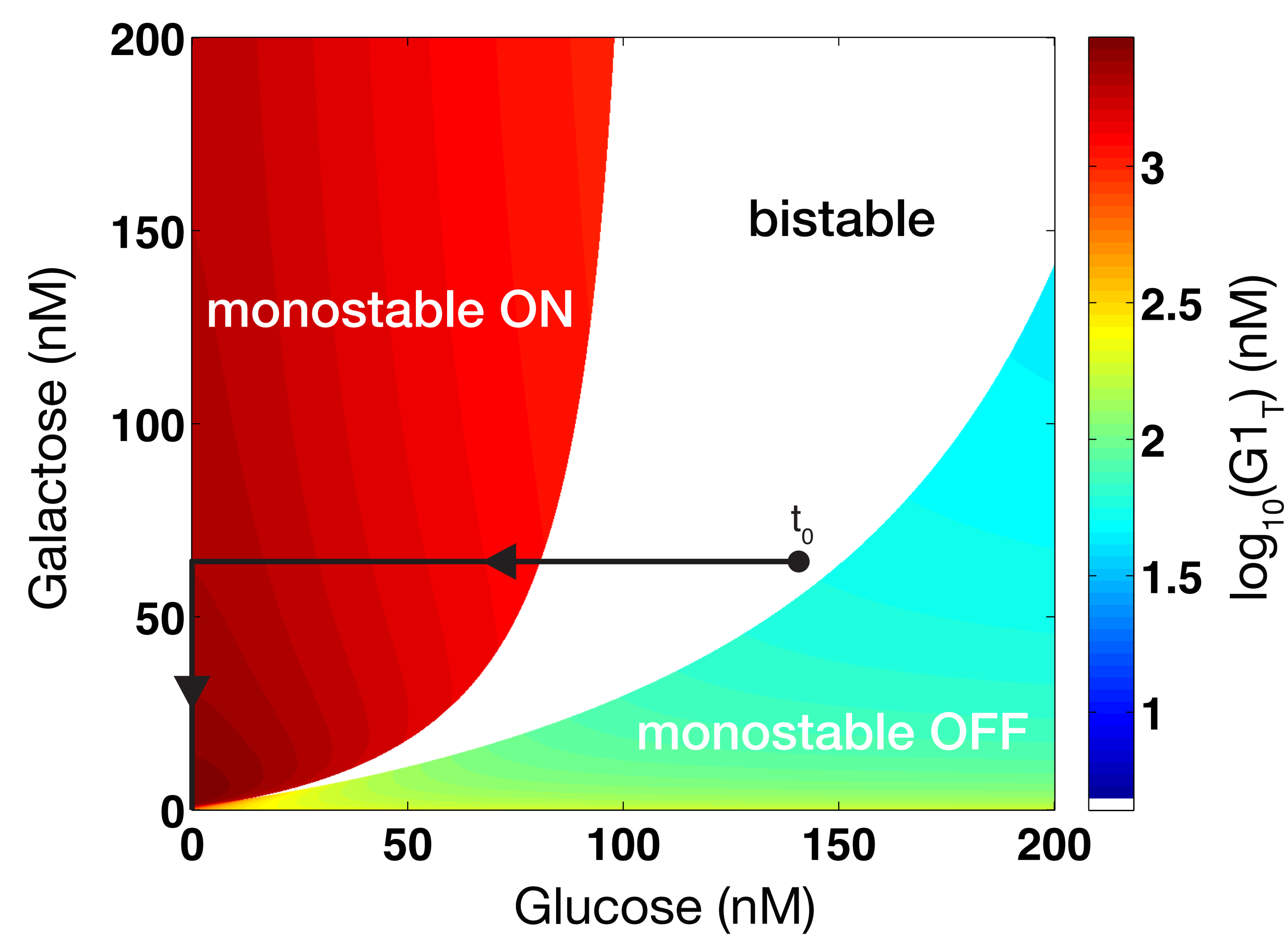

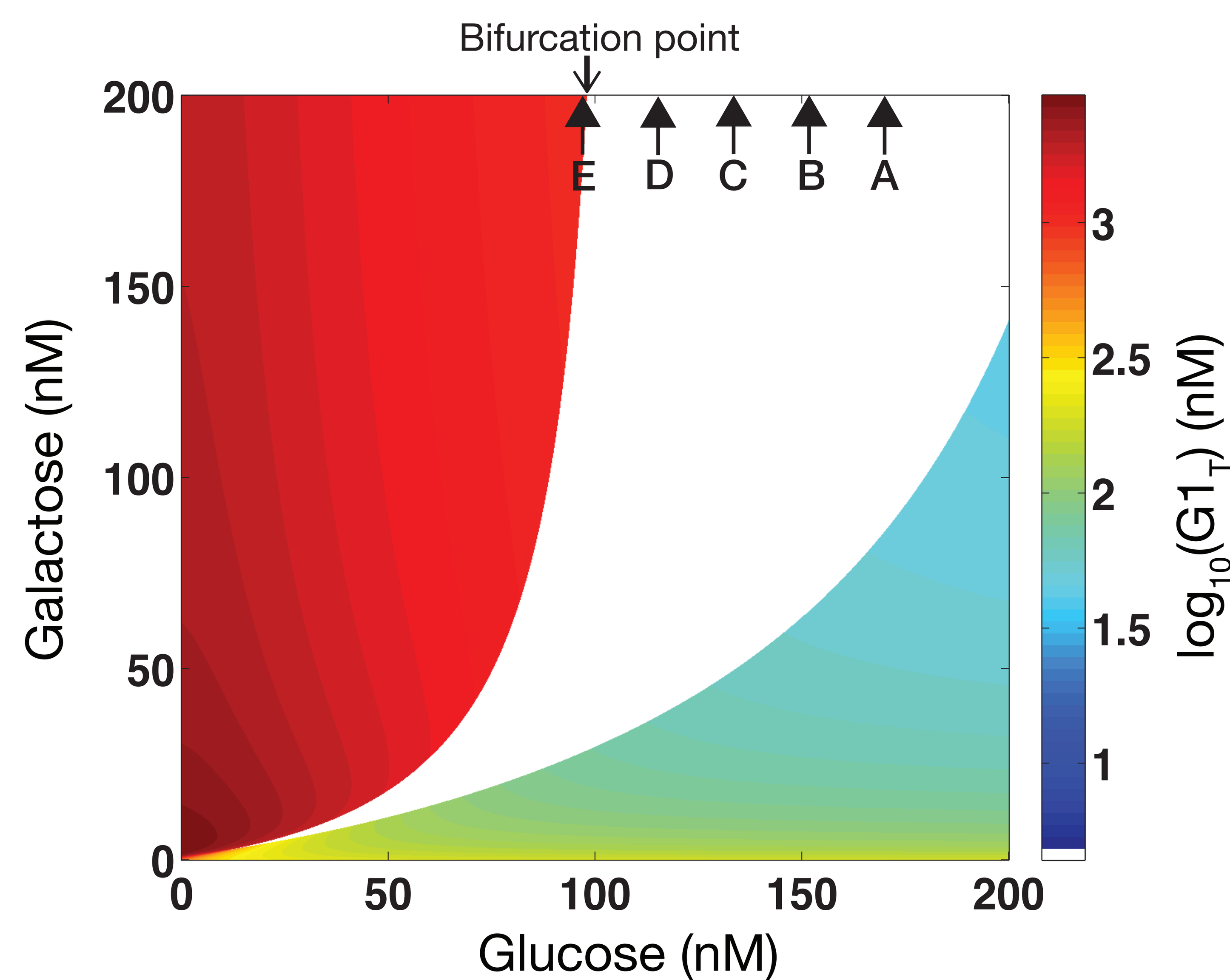

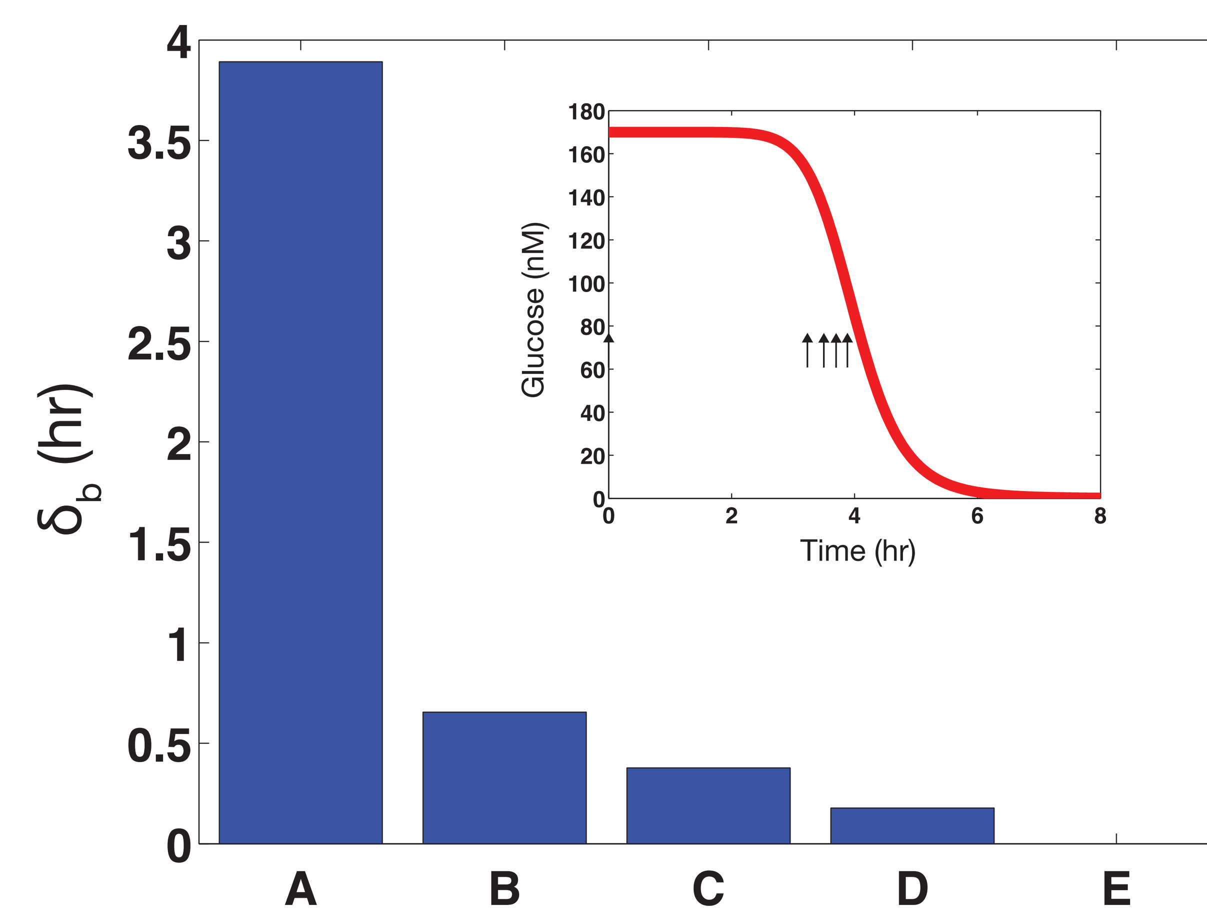

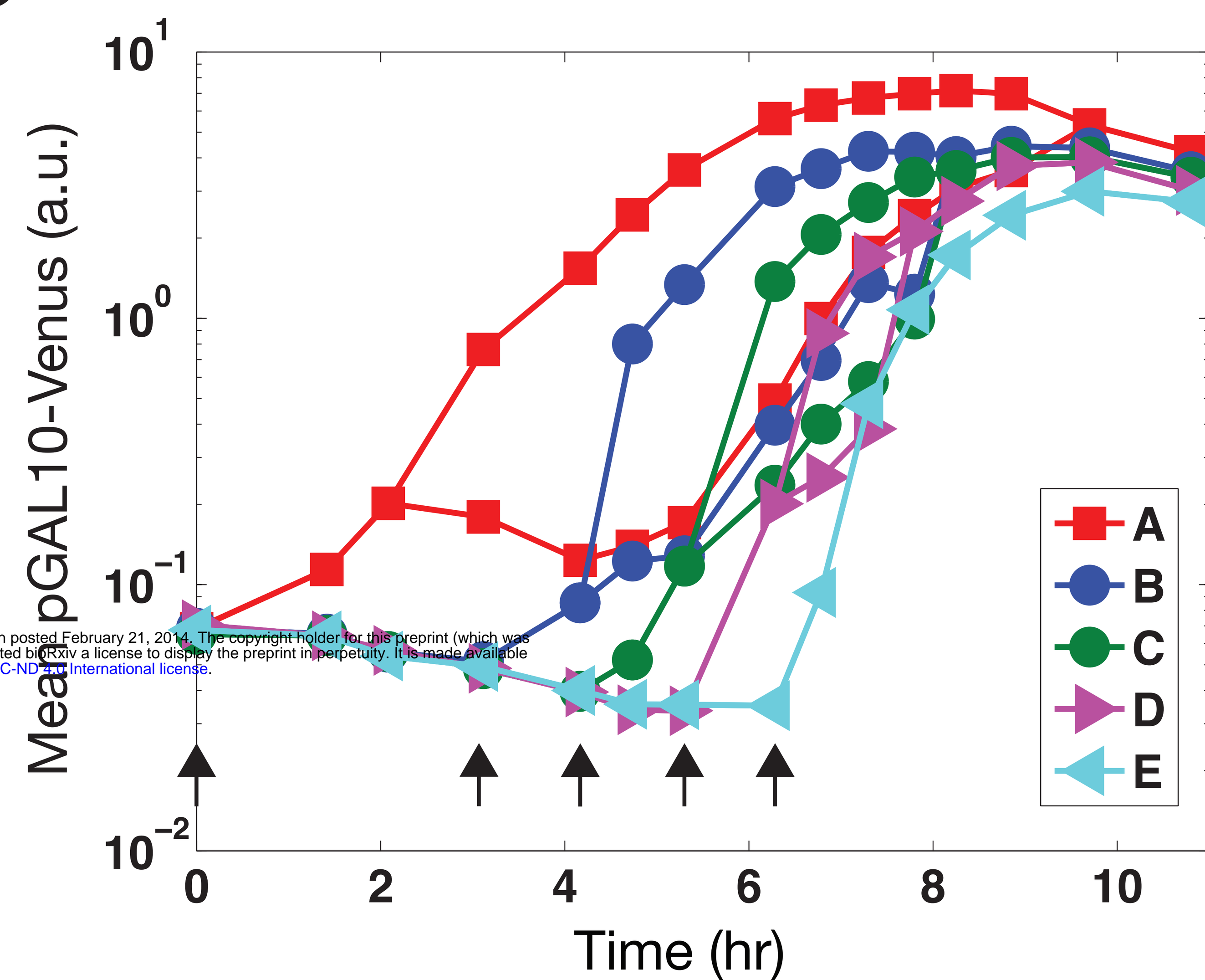

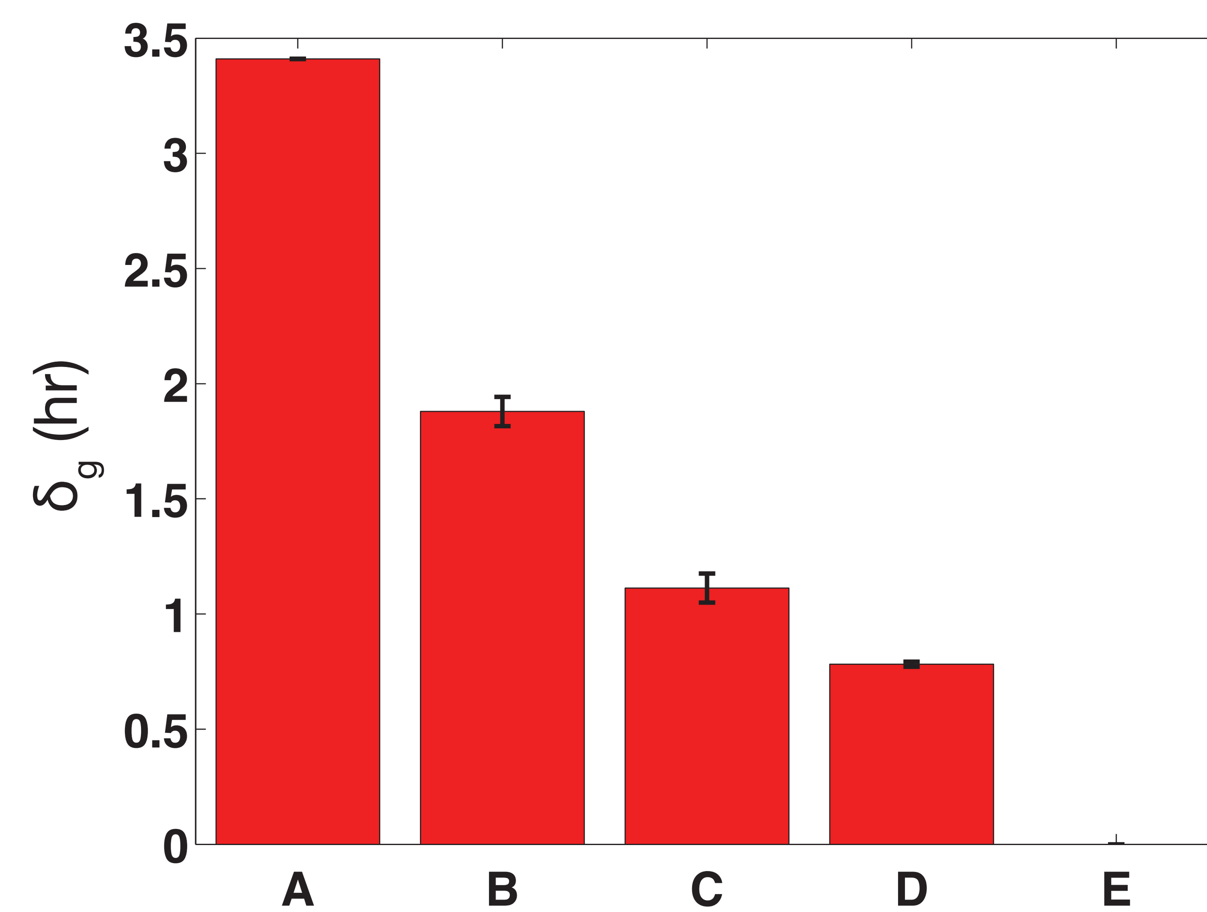

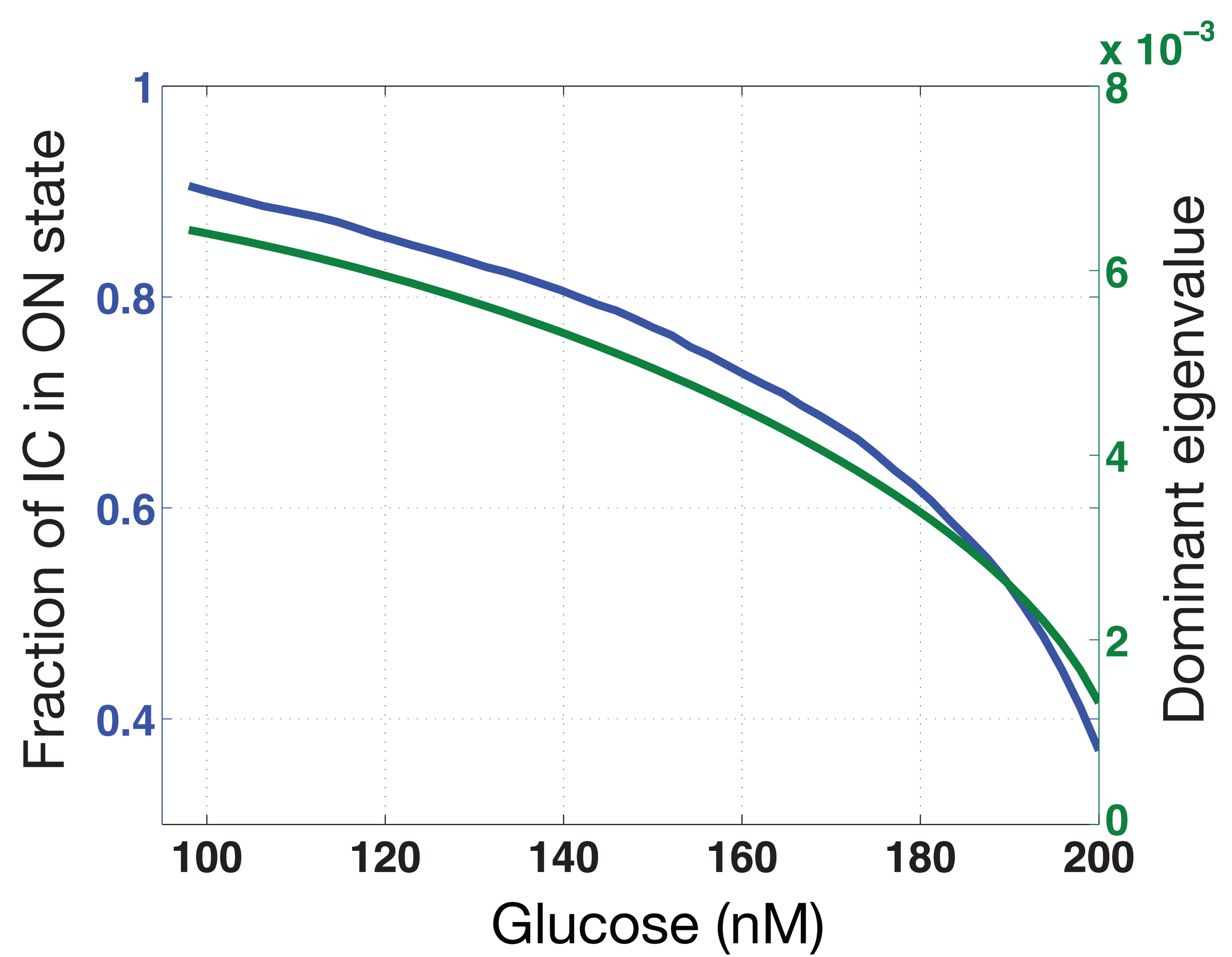

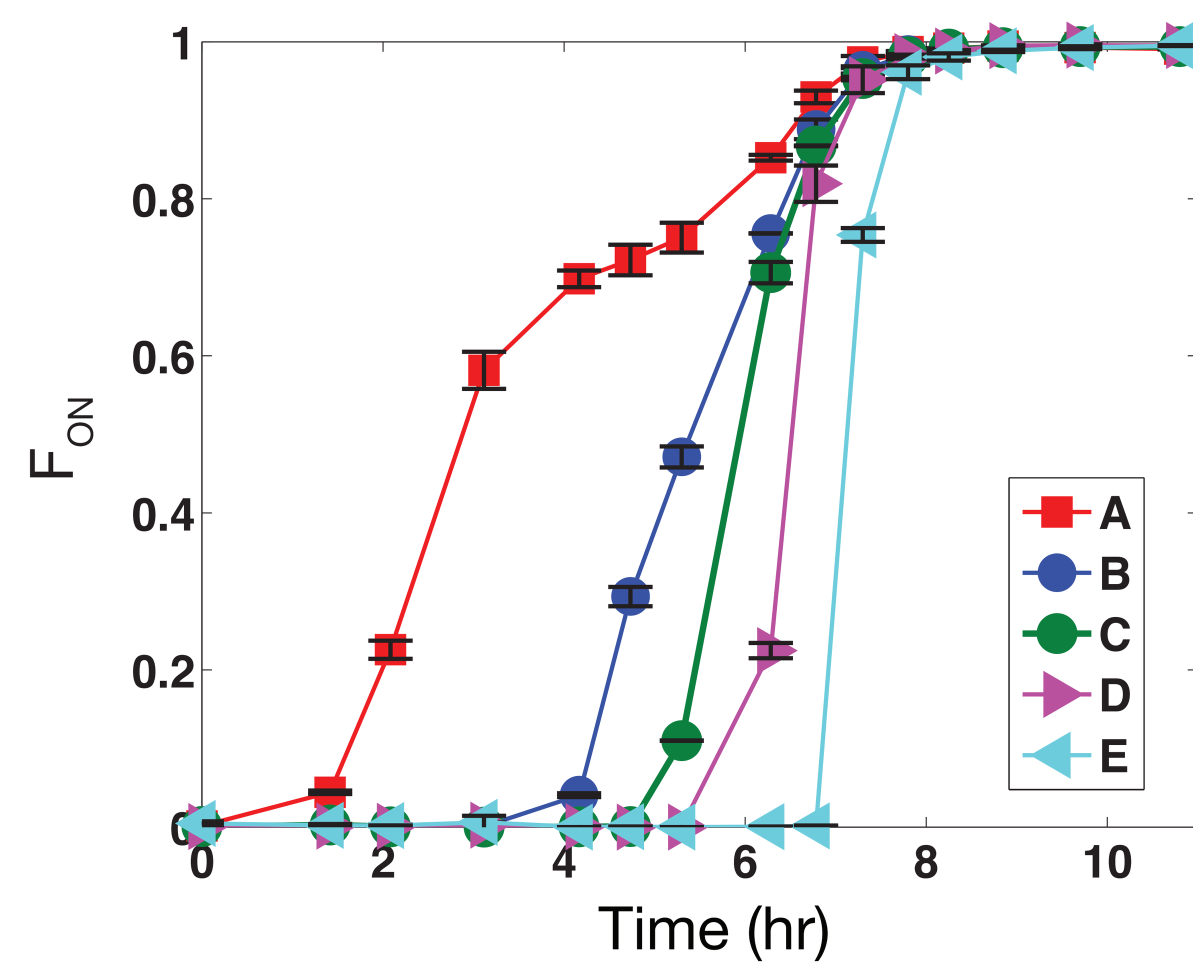

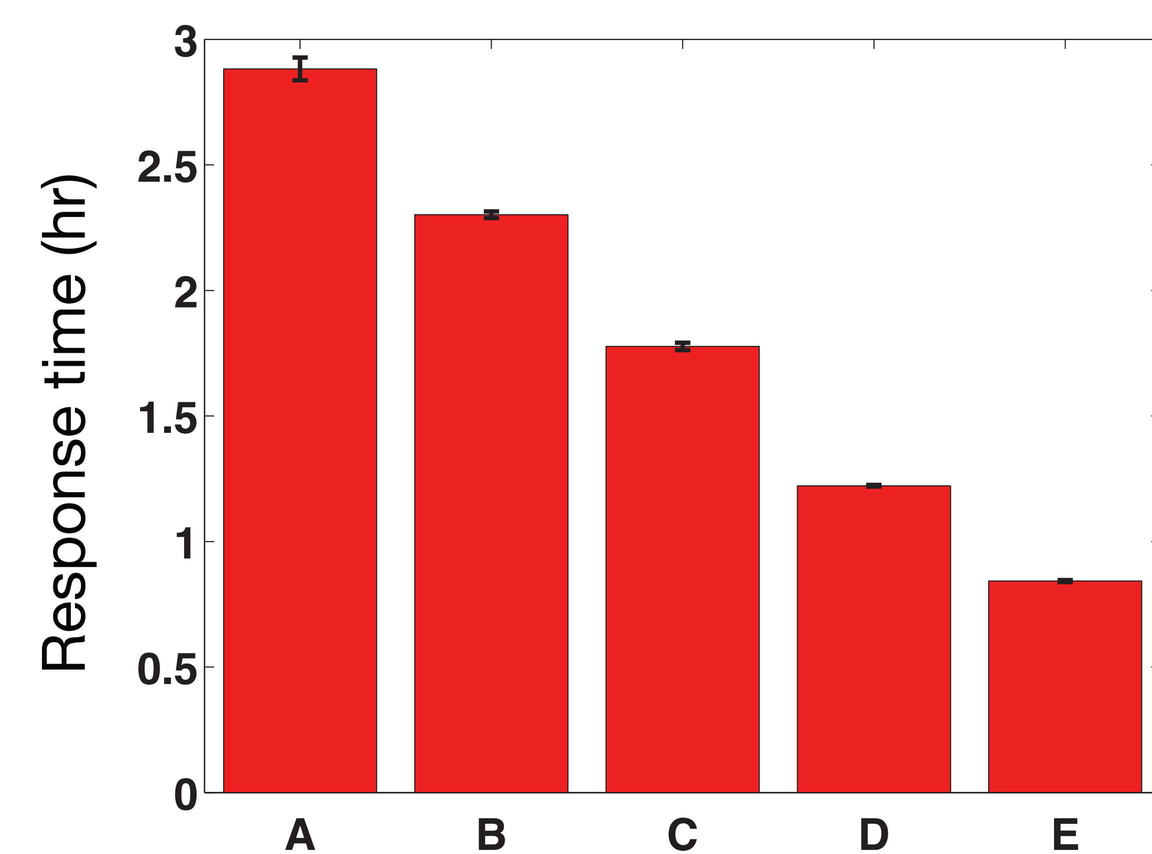

bioRxiv preprint doi: https://doi.org/10.1101/002907; this version posted February 21, 2014. The copyright holder for this preprint (which was not certified by peer review) is the author/funder, who has granted bioRxiv a license to display the preprint in perpetuity. It is made available under aCC-BY-NC-ND 4.0 International license.

bioRxiv preprint doi: https://doi.org/10.1101/002907; this version posted February 21, 2014. The copyright holder for this preprint (which was not certified by peer review) is the author/funder, who has granted bioRxiv a license to display the preprint in perpetuity. It is made available under aCC-BY-NC-ND 4.0 International license.